SLEEPING BEAUTY MEDIATED TARGETING OF TUMOR ENDOTHELIAL MARKER 8 IN THE TUMOR VASCULATURE OF COLORECTAL CARCINOMAS IN MICE

By

STEPHEN JOHN FERNANDO

A DISSERTATION PRESENTED TO THE GRADUATE SCHOOL
OF THE UNIVERSITY OF FLORIDA IN PARTIAL FULFILLMENT
OF THE REQUIREMENTS FOR THE DEGREE OF
DOCTOR OF PHILOSOPHY

UNIVERSITY OF FLORIDA

2009

To my family and friends both past and present

ACKNOWLEDGMENTS

I would like to express my sincere thanks to my mentor, Dr. Fletcher, for accepting me into his lab and giving me a project that captured my imagination and honed my skills as a researcher. His temperament, guidance, and thorough familiarity in all areas of science were crucial in the completion of my work. In addition, I would like to acknowledge the many undergraduate volunteers that made my long hours in lab more interesting as well as our technician Toni Sandlin for stoically and without complaint completing many vital tasks around the lab. Without their presence, these four and a half years would have dragged more slowly.

I offer special thanks to my committee members Drs. Siemann, Raizada, Scott and Sayeski for their direction and advice during my committee meetings. Without their help, a lot of this work would not have been possible.

I would also like to thank those who took the time to help me throughout the years because they are good people. From this group I especially thank Clive Barker, Marcus Moore and Matt Parker of Dr. Atkinson's lab, Marda Jorgenson, and the staff of the Department of Pharmacology office R5-234. Without the help of these people, the completion of my doctoral work would have been a more arduous process.

Last, but not least, I thank my family. My parents and my brother have always been there for me throughout the years. I know their support is unconditional and that I can always count on them. Finally, I thank my wife, Monica, for her unyielding love and tremendous support.

TABLE OF CONTENTS

page

LIST OF TABLES

LIST OF FIGURES

Abstract of Dissertation Presented to the Graduate School
of the University of Florida in Partial Fulfillment of the
Requirements for the Degree of Doctor of Philosophy

SLEEPING BEAUTY MEDIATED TARGETING OF TEM8 IN THE TUMOR VASCULATURE OF COLORECTAL CARCINOMAS IN MICE

By

Stephen John Fernando

May 2009

Chair: Bradley Fletcher
Major:Medical Sciences – Physiology and Pharmacology

Recent advances in cancer research have broaden the knowledge of how solid tumors progress. Once thought of as the product of a single aberrant cell with multiple mutations, tumors are the product of that single cell dividing, and then the new mass interacting with multiple nonmalignant cell types that guide its growth. Some studies examined the expression profiles of the nonmalignant cell types that associate with tumors and compared their profile to the same cell type in normal tissues. The results showed that the cells associating with the tumors expressed abnormal proteins.

Tumor Endothelial Marker 8 (TEM8) is a recently described protein preferentially expressed on tumor associated endothelial cells. The role played by TEM8 in endothelial biology remains unclear, yet this protein may allow specific delivery of therapy to tumor endothelium. This research describes the creation of a fusion protein that specifically targets TEM8 to deliver a potent vascular disrupting agent to tumor vessels.

Western blot analysis, enzyme-linked immunosorbent assays and enzymatic assays evaluated the specificity and function of the fusion proteins *in vitro*. *In vivo* analysis utilized a xenograft model of colorectal carcinoma to test the efficacy of targeted and control fusion proteins after gene delivery with Sleeping Beauty. Tumor growth curves as well as survival

studies evaluated animals receiving gene delivery of the various fusion proteins. Histology and immunohistochemistry visualized the expression and homing of the fusion proteins to the tumor vasculature, as well as effects on tumor vessel density and thrombosis.

In vitro analysis confirmed the predicted antigen specificity and function of the fusion proteins. Mice treated with the gene encoding anti-TEM8/tTF exhibited a 55% reduction in tumor volume when compared to the untreated animals ($p < 0.001$) and achieved a 49% increase in tumor growth delay by Kaplan Meier analysis ($p = 0.0367$). Immunohistochemistry confirmed tumor endothelial expression of TEM8, fusion protein homing to tumor vasculature, a decrease in vessel density and localized areas of thrombosis. Collectively, the results presented in this study indicate that targeting TEM8 is a viable anti-tumor strategy that deserves further consideration and development.

CHAPTER 1
INTRODUCTION AND BACKGROUND

Introduction

Cancer is the second leading cause of death in the United States accounting for 25% of all mortalities, and 1.5 million new cases of invasive cancer will be diagnosed this year (1). This number translates into a US male having a 1:2 chance of developing some form of an invasive cancer in his lifetime while a US female has a 1:3 chance (1). Though these numbers seem bleak, cancer treatment has improved vastly from just 30 years ago (1). In the 1970s, the five year survival rate for an invasive cancer was 50% (1). Today, that number has jumped up to 66% and for a number of cancers, the 5-year survival rates are as high as 90%(1). This increase in the 5 year survival rate is directly attributable to medical research creating tools for earlier diagnosis and improving treatments (1). Unfortunately, despite all the progress, the fact remains that cancer incidence worldwide is on the rise, and there are still forms of cancer in which the prognosis is very poor (1). As a result, new therapies are needed to treat these conditions.

Cancer Therapies Past, Present and Future

Cancer is a disease defined by uncontrolled cell growth with local and metastatic spread. The ability of cancer to spread eventually leads to death by impeding normal organ function. Classical treatments for cancer include resection, radiotherapy and chemotherapy. Resection is the best option for cancer treatment as this approach removes all or part of the malignancy and represents a clear path to a possible cure (2). However, the likelihood of this option being curative is based on tumor size, location and stage of disease (2). In many cases the tumor is inoperable or only partially operable and resection is followed by chemotherapy and/or radiotherapy (2).

Radiotherapy is an effective tool against malignancies that have high growth fractions. Radiotherapy uses high-energy waves, such as x-rays, gamma rays or photons, to cause cellular damage to cells in the involved field. This option represents an alternative to resection when the tumor is inoperable or as a supplement to resection when the tumor is only partially removed. The downside to radiotherapy is the damage the radiation causes to normal tissue, which has been minimized by improved delivery techniques (3). Application of this treatment depends on the general health of the patient, tumor location, stage of disease and type of cancer (3). Radiation is not considered effective against highly metastatic tumors limiting the effectiveness of this option in many late-stage patients.

Chemotherapy refers to a group of drugs that is given to patients to treat cancer. Generic categories for chemotherapy agents include antimetabolites, genotoxic drugs, spindle inhibitors and DNA synthesis inhibitors. Antimetabolites include drugs like 5-fluorouracil where the method of action is to interfere with the production of essential molecules such as nucleic acids for RNA and DNA synthesis. Genotoxic drugs damage DNA and include categories of drugs like alkylating agents, intercalating agents, and enzyme inhibitors. An example of a genotoxic drug is cisplatin, which causes crosslinking of the DNA strands. Spindle inhibitors prevent cell division and lead to cell death. Their method of action targets the microtubules that are essential proteins involved in chromosome separation during mitosis. An example of a spindle inhibitor is paclitaxel, which is derived from the bark of the Pacific Yew tree. DNA synthesis inhibitors block DNA synthesis and cause cell death although the exact mechanism by which some of these drugs work remains unknown. An example of a DNA synthesis inhibitor is bleomycin, which is a protein, isolated from the bacterium *Streptomyces verticullis*. Chemotherapy is used alone or often in combination with radiotherapy and/or resection to treat malignancies. The main

drawback to chemotherapy are the side effects caused by the drugs which vary by treatment dose and patient issues, and can range from innocuous to life threatening (4, 5). These negative side effects occur because chemotherapy cannot discriminate malignant cells from normal rapidly dividing cells such as cells in the bone marrow and cells lining mucosal membranes (4, 5). Liver and renal cells which are responsible for chemical breakdown and excretion can also be negatively impacted (4, 5).

Although chemotherapy, radiotherapy and resection represent the cornerstone of cancer treatment, these treatments have been joined recently by hormonal therapy, biological therapy, and targeted therapy. These newer therapies are the result of medical research providing a better understanding of cancer at a molecular level. Though these newer treatments by themselves generally are incapable of curing malignancies, they have been shown to increase survival time and quality of life. Hormone treatment is based on the idea that cancer cells are dependent on hormonal signals to grow. The drugs used in this therapy either block hormone signaling in target cells or prevent hormone production. Unlike the earlier described therapies, hormone therapy is mainly limited to breast (6), ovarian (7) and prostate cancer (8). Biological therapy involves artificially enhancing the body's natural immune response to cancer (9). There are two general approaches used in biological therapy (9). The first approach utilizes the use of cytokines which are proteins used to communicate within and between cell types. Cytokines such as interleukin-2 and alpha interferon are immunostimulatory and they increase the body's natural immune response to tumor cells (9). The second approach in biological therapy involves the use of monoclonal antibodies like trastuzumab (Herceptin) (10). Monoclonal antibodies bind specific targets at high affinity, which can result in the disruption of downstream signaling or proteolytic cleavage of bound receptors leading to a reduction in tumor growth and even tumor

cell death. Targeted therapy uses small molecules or proteins to directly target cellular processes predominately used by cancer cells (11). This new approach is very attractive since these drugs are inherently not toxic and are more specific for cancer cells. Two of the more celebrated drugs in this category include imatinib (12) and bevacizumab (13). Targeted therapy is an area of incredible potential even though the specificity of targeted therapy is also its immediate drawback. Targeting one pathway in cancer is usually not enough to defeat the disease, and the chance of developing resistance is higher if only a single drug is used.

Resistance to treatment is an area of growing interest in cancer therapy. The high rate of mutation in malignancy creates a heterogeneous population of cells within the tumors. Some of these cells can overcome therapy by relying upon redundant pathways for growth and spread (14). This problem directly leads to disease relapse and eventually end-stage symptoms if other treatments are ineffective. This unfortunate attribute of cancer cells highlights the importance of advancing research in cancer biology so we can ascertain new targets for therapy and develop innovative drugs that specifically target malignant cells and are minimally toxic to normal cells. A primary focus of this work was to create a new cancer therapy that targets a novel and relevant cancer antigen. To satisfy this goal, we looked at an innovating area of cancer research that examines the entire tumor microenvironment rather than just tumor cells.

Tumor Microenvironment

For years, cancer research centered on the cancer cell and the abnormal internal pathways they use to grow, spread and evade normal homeostasis. This research discovered that mutations to oncogenes and loss of function to tumor suppressor genes resulted in phenotypes characterized as cancer (15). This original research on cancer biology drove the early advancements and combinatorial strategies that have become the cornerstone of cancer therapy treatments. However, a new area of cancer research has developed that goes beyond the cancer cell and

considers the relationship between nonmalignant stromal cells and cancer cells. The interaction of nonmalignant cells and tumor cells is termed the tumor microenvironment, and the nonmalignant cell types include fibroblasts, glial, epithelial, fat, immune, smooth muscle and vascular cells (16). Research on the tumor microenvironment has focused mainly on fibroblasts, immune cells and vascular cells. How the tumor microenvironment develops and what regulated its formation is an area of intense research. Current evidence indicates tumor cells control the microenvironment and influence stromal cells to provide supporting structure (16).

An important cell type found within the tumor microenvironment are the immune cells. Immune cells innately target cancer cells via a T-cell mediated response (16). Tumor markers or the renewed expression of embryonic specific proteins are thought to help initiate this response. However, the tumor has developed ways to circumvent the immune system by recruiting regulatory T-cells, macrophages and myeloid suppressor cells which secrete cytokines IL-10 and TGF-β (16). These cytokines inhibit the expansion of tumor targeting T-cells, the maturation of dendritic cells and other lymphocyte mediated anti-tumor responses (16). Ironically, the initial immune response helps the tumor grow by creating an environment resembling that of a new wound. This type of environment is pro-angiogenic and pro-growth and attracts a number of specialized cells including activated fibroblasts.

Fibroblasts are another component of the tumor microenvironment that actively provides support for the tumor. Fibroblasts are the majority nonmalignant cell type in the tumor microenvironment and they provide the most support for tumor growth (17). Cancer associated fibroblasts (CAF) are activated fibroblasts; meaning, they exhibit a rare fibroblast phenotype that is reserved for instances of regeneration like wound healing (17). These activated fibroblasts secrete growth factors that induce vessel formation and promote cell growth in order to repair

lesions (17). Once the lesions are healed, they are eliminated from the area by differentiation or apoptosis. CAFs mimic this phenotype, but instead of being eliminated once needs are met, they continue to release pro- growth and pro-angiogenic factors (18). This constant stimulation for growth and angiogenesis results in the initiation of the tumor vessel network (17).

In order to grow beyond the size of 2-3$mm^3$and gain metastatic potential, tumors must recruit blood vessels to relieve the nutrient deprived and hypoxic conditions created by uncontrolled cell growth (19, 20). Tumors vessels can form by three different mechanisms which include vessel sprouting from existing vasculature (angiogenesis), recruitment of vascular progenitor cells that create new vessels (vasculogenesis) or vascular mimicry, which entails tumor cells lining tubules that join to the vascular network (20, 21). Unlike normal vessels, tumor vessels are leaky and disorganized (22). This tortuous arrangement is a result of constant stimulation by the tumor cells and the supporting stroma to grow (22). Another consequence of this constant growth stimulation is the aberrant expression of proteins on the surface of the stromal cells in the tumor microenvironment much like the expression of tumor markers on tumor cells (23-25).

Tumor markers are upregulated proteins found on the surface or released by tumor cells because of their malignant phenotype and tissue of origin. These markers generally provide a survival advantage to the tumor cell or represent an embryological marker. An example of a tumor marker is carcinoembryonic antigen (CEA) (26). Carcinoembryonic antigen is a tumor cell marker of epithelial origin best characterized in colorectal carcinomas. Its expression is limited in normal tissue and elevations in serum concentration are an indicator of serious disease which is usually a malignancy (27), but could also be ulcerative colitis, pancreatitis or cirrhosis (28). Carcinoembryonic antigen overexpression confers a resistance to anoikis and enhances

metastasis potential (26). Anoikis is programmed cell death due to detachment from the extracellular matrix. Carcinoembryonic antigen was one of the first described tumor markers and analysis of CEA expression/presence is still used today to detect tumors and to evaluate the effectiveness of anticancer therapies.

Determining tumor stromal markers and the pathways they promote is a developing area of cancer research that can provide new leads for targeted therapies. Reports trying to elucidate tumor stromal markers have used techniques like suppression subtraction hybridization (25), microarray (23) and serial analysis of gene expression (SAGE) (24). These techniques can examine the differential expression of proteins in normal versus malignant tissues. The cell type most often studied in these reports are tumor associated endothelial cells. The reason endothelial cells are prominent in this type of research is the importance the vessel network plays in tumor growth and eventual metastasis (20, 21). Discovering markers on these endothelial cells can lead to therapies that damage tumor vessels and lead to a decrease in malignant progression. Several promising candidate genes have been identified and one such protein is tumor endothelial marker 8 (TEM8) (24).

Tumor Endothelial Marker 8

Tumor Endothelial Marker 8 is a type-1-transmembrane protein with an extracellular von Willebrand factor-like domain and a metal-ion dependent adhesion site (MIDAS) (29). The exact physiological function of TEM8 remains unknown, but it is one of two known proteins capable of facilitating anthrax toxin entry into cells (30, 31). *In vitro* studies on TEM8 function indicate a role in endothelial cell adhesion, migration, and capillary tubule formation(32-34). The extracellular domain of TEM8 can bind to collagens type I (32) and VI (35), as well as protective antigen (PA) (30) of the anthrax toxin, while the cytosolic domain interacts with actin and has several possible phosphorylation sites that could be involved in cell signaling (29, 36).

These results are consistent with the type-1-transmembrane protein structure of TEM8 and suggest a function in cell-matrix interactions (29, 37).

Expression profiles for TEM8 include both research and clinical samples and both provide strong evidence for the presence of TEM8 in tumor endothelial cells. *In vitro* studies show endothelial cells co-cultured with tumor cells or exposed to tumor conditioned medium up-regulate TEM8 (38). Clinical samples showed TEM8 expression at both the transcript and protein level associates with stage of disease in colorectal carcinoma and breast cancer (39-42). Tumor Endothelial Marker 8 expression was also detected in the vessels of various human malignancies by *in situ* hybridization (35). In normal adult tissues, TEM8 expression is sporadic and found at lower levels than in tumor endothelium (35, 40). No reports show constitutive TEM8 expression in normal adult endothelial cells, but expression was found in human umbilical cord endothelial cells (32), endothelial cells of infantile hemangioma (43) and in vessels during murine embryonic development (29). These results suggest TEM8 is a novel endothelial marker that may have therapeutic applications by allowing targeting of tumor endothelium.

Three recent articles supported the idea that TEM8 is an important target in tumor progression. Two of these articles utilized components of the anthrax toxin to target tumors *in vivo*. The third paper fused the extracellular domain of TEM8 to the constant region of IgG1 and administered the fusion protein systemically (44). Collectively, the results showed that targeting anthrax toxin receptors or blocking TEM8 from interacting with a physiological partner in solid tumors slowed tumor growth and resulted in a decrease in tumor vessel density (44-46). These experiments did not demonstrate specific targeting of TEM8, as anthrax toxin is also known to bind the related protein CMG2, but they do support the idea that strategies targeting TEM8 or keep it from binding a physiological partner are effective and warrant further investigation.

Research Overview

The goal of this research was to create a therapy that specifically binds TEM8 and uses this affinity to deliver a potent vascular disrupting agent to tumor vessels. To achieve this goal, a gene delivery-based approach was used to target TEM8 in tumor vessels and to disrupt existing tumor vasculature by promoting thrombosis. The approach involved the synthesis of a gene encoding a novel fusion protein. The N-terminal domain of the fusion protein is a single-chain antibody (47) that binds to the extracellular domain of TEM8 allowing for targeting. The C-terminal domain is an effector domain that encodes truncated tissue factor (tTF) (48) with the goal of initiating localized thrombosis events within the tumor vasculature. We compared the results achieved by targeting TEM8 to that of a similar fusion protein that targets the established tumor marker CEA as well as a nonspecific fusion protein. Targeting CEA to deliver truncated tissue factor and occlude tumor vasculature relied upon the leaky and disorganized nature of tumor vessels and assumes the tissue factor domain will still promote thrombosis even though it may not accumulate within the vessel. The gene encoding each fusion protein was placed inside a Sleeping Beauty vector to facilitate gene integration and long-term expression.

Chapter 2 describes the experimental procedures used to complete this doctoral research. Chapter 3 details the background and history of the Sleeping Beauty Transposon system as well as the current and future uses of this system in medicine. Sleeping Beauty is the vector of choice within our lab and it represents a novel alternative to both purified protein delivery and viral mediated gene delivery.

In Chapter 4, the creation of the fusion protein genes and the *in vitro* characterization of the fusion proteins are described. Proper assembly, expression, secretion and function of the fusion proteins are an important aspect of this doctoral research. In addition, confirming the

activity of the fusion proteins is a necessary prerequisite for testing of the therapies in a xenograft model.

Chapter 5 evaluates the therapies in a xenograft model of colorectal cancer. A Sleeping Beauty vector carrying the gene for each fusion protein was administered to a separate group of mice and the effect of each therapy was quantified and compared to an untreated control. In addition, the tumors are excised an examined to confirm fusion protein localization and thrombosis within the tumor. The results of the *in vivo* experiments are discussed in this chapter as well as their place in the literature.

Finally, Chapter 6 highlights the major findings of this research and provides suggestions for future directions.

CHAPTER 2
MATERIALS AND METHODS

Cell Culture

All cell lines were grown in Dulbecco's Modified Eagle Medium high glucose (Gibco, Invitrogen Corporation, Carlsbad, CA) supplemented with 1% penicillin-streptomycin-glutamine (Gibco Invitrogen Corporation, Carlsbad, CA) and 10% Fetal Bovine Serum (FBS) except the murine hybridoma cell line, HB-8747 (ATCC, Manassas, VA) which required 20% FBS. Cells were grown at 37°C in 5% CO_2 until 80% confluence was reached. Cells were unattached from plates using trypsin and split 1:10 with fresh medium.

Cloning and Expression of TEM8 and CMG2

Reverse transcriptase polymerase chain reaction (RT-PCR) was used to obtain the cDNA for TEM8 and CMG2 using the Titan One Tube System (Roche, Indianapolis, IN). mRNA was obtained from Hela cells and C166 mouse endothelial cells for TEM8 and CMG2 respectively using Trizol Reagent (Invitrogen Corporation, Carlsbad, CA). The sense primer for TEM8 was 5'-ATGGCCACGGCGGAGCG-3' and the antisense primer was 5'-GACAGAAGGCCTTGGAGGAGGGC-3'. For CMG2, the sense primer was 5'-ATGGTGGCCGGTCGGTCC-3' and the antisense primer was 5'-TTATTGATGTGGAACCCGGGAG-3'. The conditions used to generate the cDNAs for TEM8 and CMG2 were as follows: 30 minutes at 50°C, followed by 5 minutes at 94°C, followed by 25 rounds of 94°C for 1 minute, 50°C for 30 seconds and then 72°C for 2 minutes; the final extension time was for 10 minutes at 72°C. The cDNAs were cloned into the shuttle vector pCR4-TOPO (Invitrogen Corporation, Carlsbad, CA) and cut out via *EcoRI* (New England Biolabs, Ipswich, MA) digestion. Next, the cDNAs were individually placed into the retroviral plasmid pBMN/IRES-GFP, which links protein expression to GFP and allows for FACS Sorting.

The pBMN/IRES-TEM8/GFP or pBMN/IRES-CMG2/GFP plasmids were separately transfected into the Phoenix A packaging cell line. Retrovirus was used to infect 293T cells and create the two 293T cell lines that overexpress either TEM8 or CMG2. The cell lines were enriched by FACS sorting of GFP positive cells and after two rounds of sorting were approximately 99% GFP positive. Confirmation of the 293T/TEM8 cell line was established by Western blot analysis via the SB5 monoclonal antibody to TEM8 compared to uninfected 293T cells. The 293T/CMG2 cell line was confirmed by semi-quantitative RT-PCR compared to control cells, as an antibody specific for CMG2 is not available.

Parental Monoclonal Antibody SB5 Specificity

The cell lines 293T, 293T/TEM8 and 293T/CMG2 were grown in 6cm dishes for 48 hours. The cells were washed twice with ice-cold phosphate buffered saline (PBS) and lysed by addition of sample application buffer (62.5mM Tris, 10.0% Glycerol, 3.0% SDS, pH 6.8). Samples were homogenized by passage through a 30-gauge needle. Protein concentrations were determined using the BCA protein assay (Pierce, Rockford, IL). 30 μg of protein was loaded on 10% SDS-PAGE gel and transferred to a polyvinylidene difluoride (PVDF) membrane overnight at conditions of 4°C, 0.10mA. The next day, samples were blocked with milk buffer (milk powder 5% in PBS + 0.01% Tween 20, 10% FBS) and probed with the SB5 monoclonal antibody at a dilution of 1/1000. Detection was performed with a goat anti-mouse horseradish peroxidase (HRP) conjugated secondary antibody (Abcam, Cambridge, MA).

Fusion Protein Construction and Cloning into the Sleeping Beauty Transposon System

Cloning the Anti-TEM8 Variable Regions

First strand cDNA and mRNA from the SB5 monoclonal antibody hybridoma were a kind gift from the laboratory of Dr. Brad St. Croix as well as information that SB5 was a murine IgG1 antibody with a kappa light chain. Using this information, we captured the sequences of the

variable light and heavy chain of SB5 using a 5` RACE kit (Invitrogen Corporation, Carlsbad, CA) basing our gene specific primers (GSP) on published sequences of both the CH1 domain of murine IgG1 and areas of the kappa light chain constant region that are conserved. The gene specific primers (GSPs) used for the variable light chain were GSP1, 5'-TCAGTCCAACTGTTCAGG-3' and GSP2, 5'-GTTCACTGCCATCAATCTTCC-3'. The GSPs used for the variable heavy chain region were: GSP1, 5'-GTCACTGGCTCAGGGAAATAGC-3' and GSP2, 5'-ATCTTCTTCCTGATGGCAGTGG-3'. After 5`RACE, cloning and sequencing of the products, the DNAs were amplified again using the SB5 variable light chain primers 5'-TTAGCGGCCGCCACCATGGACATGAGGACCCCTGC-3' for sense and 5'-CGCCAGATCCGGGCTTGCCGGATCCAGAGGTGGAGCCTTTCAGCTCCAGCTTGGTCC-3' for antisense. This second amplification was done to add a *NotI* (New England Biolabs, Ipswich, MA) endonuclease site to the 5' end of the variable light chain for cloning purposes and a partial 218 linker (49) region to the 3` end (underlined regions). Secondary amplification of the heavy chain sequences was performed using the sense primer, 5'-CGGCAAGCCCGGATCTGGCGAGGATCCACCAAGGGCCAGATCCAGTTGGTGCAGTCTGA-3', and the antisense primer, 5'-CCGCCTCCGGAGCCCCCACCCCCTGCAGAGACAGTGACCAGAGTC-3'. This amplification added a partial 218 linker to the 5` end of the variable heavy chain of SB5 and a partial $(G_4S)_3$ linker (50) to the 3` end that would eventually connect the variable heavy chain to both the variable light chain and truncated tissue factor respectively (underlined regions). All primers were purchased from Integrated DNA Technologies (Coralville, IA).

Cloning the Anti-CEA Variable Regions

The mRNA for the variable light and heavy chains of the anti-CEA monoclonal antibody T84.66 was obtained from the HB-8747 hybridoma (ATCC, Manassas, VA) using Trizol Reagent. The sequence of the variable light and heavy chains of the T84.66 monoclonal antibody are published simplifying primer development (Accession Numbers X52768 and X52769). The *NotI* endonuclease site and linker regions were added to the cDNAs of the variable light and heavy chains of T84.66 in the same way as for SB5. RT-PCR was used to amplify the sequences from RNA using the following primer pairs: Sense primer of the variable light chain of T84.66 5'-TTAGCGGCCGCCACCATGGAGACAGACACACTCCTGC-3' and antisense primer 5'-CGCCAGATCCGGGCTTGCCGGATCCAGAGGTGGAGCCTTTTATTTCCAGCTTGGTCC-3'; sense primer for the variable heavy chain of T84.66 5'-CGGCAAGCCCGGATCTGGCGAGGGATCCACCAAGGGCGAGGTTCAGCTGCAGCAGTC-3' and antisense primer 5'-CCGGAGCCTCCGCCTCCGGAGCCCCCACCCCCTGAGGAGACGGTGACTGAGG-3'.

Cloning Murine Truncated Tissue Factor

The mRNA for murine truncated tissue factor was obtained from brain tissue of a C57Bl/6 mouse using Trizol Reagent and RT-PCR. The sense primer used was 5'-GCTCCGGAGGCGGAGGCTCCGGAGGAGGCGGGTCCATGGCGATCCTCGTGCGCC-3' which added a partial (G4S)3 linker region to the 5` end of truncated tissue factor and the antisense primer used was 5'-TTAGCGGCCGCTCAGCAGTAGCTTACTCCTTCTTCCACTTA-3' which added a *NotI* endonuclease site used in subsequent cloning steps. A final primer was used to add the mycHis tag to the 3' ends of DNA encoding the fusion proteins 5'-

GCGGCCGCTCAATGGTGATGGTGATGGTGGTCCACGGCGCTGTTCAGGTCCTCCTCG CTGATCAGCTTCTGCTCGCCAAAGCAGTAGCTTACTCCTTC-3' with the underlined region encoding the tag and included a *NotI* endonuclease site.

Cloning the Dead-sc/tTF Fusion Protein

Dead-sc/tTF was created by removing critical amino acids within the antigen binding domains of the variable light chain of SB5 and the variable heavy chain of T84.66. The two antibody fragments were joined together to form a nonspecific single chain antibody. The modifications required two separate PCR reactions for each fragment and then the fragments were joined by SOE PCR. The fragments for the variable light chain of SB5 were created using the primers 5`-TTAGCGGCCGCCACCATGGACATGAGGACCCCTGC-3' and 5`-AAGATCTGTCCTGACTCGCCTTGC-3' to make the upper fragment and 5`-AAGATCTGGGGTCCCATCAAGGTTCC-3' and 5`-CGCCAGATCCGGGCTTGCCGGATCCAGAGGTGGAGCCTTTCAGCTCCAGCTTGGTCC -3' to make lower fragment. The underlined region represents a *BglII* site that was used to join the two fragments together. The fragments for the variable heavy chain of T84.66 were created using the primers 5`-CGGCAAGCCCGGATCTGGCGAGGGATCCACCAAGGGCGAGGTTCAGCTGCAGCAGT C-3' and 5`-CCTCGAGAATGTTGAAGCCAGAAGC-3' to make the upper fragment and 5`-CCTCGAGTTCCAGGGCAAGGCCACT-3' and 5`-GCGGCCGCTCAATGGTGATGGTGATGGTGGTCCACGGCGCTGTTCAGGTCCTCCTCG CTGATCAGCTTCTGCTCGCCAAAGCAGTAGCTTACTCCTTC-3' to make lower fragment. The underlined region represents an *XhoI* site that was used to join the two fragments together. SOE PCR was then used to join the variable regions together which contained partial overlap of the 218 linker.

Creating Anti-TEM8/tTF, Anti-CEA/tTF and Dead-sc/tTF by SOE PCR

Gene splicing by overlap extension utilizing polymerase chain reactions (SOE PCR) (51) was used to join the variable light chain regions to the variable heavy chain regions to create the anti-TEM8, anti-CEA and Dead-single chain antibodies. Then separate SOE PCR reactions were performed to join the individual scFvs to tTF using complementary regions of the $(G_4S)_3$ linker. The reaction conditions used for PCR SOE were 94°C for 10 minutes, followed by 10 cycles of 94°C for 1 minute, 45°C for 30 seconds, 72°C for 1 minute, followed by 25 cycles of 94°C for 1 minute, 55°C for 30 seconds, 72°C for 1 minute, followed by a final extension of 72°C for 10 minutes. The PCR enzyme used in these reactions was the Expand High Fidelity System (Roche, Indianapolis, IN).

General Cloning Steps

After each of the constructs were completed, the samples were run on a 0.9% agarose gel for visualization and purified using the Qiaex II procedure (Qiagen, Valencia, CA). The samples were cloned into the pCR4-TOPO shuttle vector (Invitrogen Corporation, Carlsbad, CA) and sequenced by Seqwright (Houston, TX). Following verification of sequence fidelity, the anti-TEM8/tTF, anti-CEA/tTF, and Dead-sc/tTF fusion protein constructs were cut out of pCR4-TOPO vector via *NotI* digestion and ligated into the Sleeping Beauty backbone pMSZ/CBA. The samples were checked for orientation using an *EcoRI* cut and correct samples were amplified using an Endo-Free Giga Prep Kit (Qiagen, Valencia, CA) for subsequent experiments.

In Vitro Characterization of the Fusion Proteins

Expression and Secretion

Proper production, secretion and function of the fusion proteins were verified by calcium phosphate transfections (52) (52)in 293T cells using the Sleeping Beauty vectors pMSZ/CBA-anti-TEM8/tTF, -anti-CEA/tTF or -Dead-sc/tTF. To show production and secretion, 6 cm tissue

culture dishes were seeded with 2 X 10^6 293T cells. The next day, the cells were transfected with the specific plasmids. The transfected cells were incubated for 72 hours post-transfection and then aliquots of the medium and cell lysate were collected for Western blot analysis to verify production and secretion.

To isolate partially purified proteins, medium was passed through a 0.2 μm filter (Thermo Fisher Scientific, Rochester, NY) and resuspended 1:1 with lysis buffer (50mM NaH2PO4, 300mM NaCl, 10mM imidazole pH 8.0). The final pH of the solution was adjusted to 8.0 using 10N NaOH. Next, the solution was mixed with 0.25mL of Ni-NTA agarose (Qiagen, Valencia, CA) and shaken at 4°C at 200 rpm for 2 hours. The samples were passed through a disposable column and washed twice with 4mL of wash buffer (50mM NaH2PO4, 300mM NaCl, 20mM imidazole pH 8.0) and then eluted with 2mL of elution buffer (50mM NaH2PO4, 300mM NaCl, 250mM imidazole pH8.0). Samples were then concentrated using an Amicon® 30 cartridge (Millipore, Billerica, MA) to final volume of ~200 μL. The cell lysates were collected in 0.3mL of sample application buffer. Next, 30 μg of cell lysate or 25 μL of Ni-NTA (Qiagen, Valencia, CA) purified fusion protein were combined with loading buffer, boiled and loaded on two 10% SDS-PAGE gels. Samples were transferred to a PVDF membrane and the membranes were probed either with an HRP-conjugated anti-His antibody (Invitrogen Corporation, Carlsbad, CA) or with a rabbit anti-murine tissue factor antibody (American Diagnostica, Stamford, CT) and a goat anti-rabbit HRP-conjugated secondary antibody. Immunoreactive bands were illuminated using Western Lightning solution (PerkinElmer, Waltham, MA).

Anti-CEA/tTF Binding

CEA binding by indirect ELISA

The binding specificity for the anti-CEA fusion protein was demonstrated using an indirect ELISA assay. Briefly, maxisorp microtiter plates (Thermo Fisher Scientific, Rochester, NY)

were coated with 100 µL of purified CEA protein (Abcam, Cambridge, MA), at a concentration of 4 µg/mL at 4ºC overnight. The wells were washed three times for 5 minutes with 400 µl PBST (PBS + 0.01% Tween 20). Each well was then blocked with 200 µL of PBST + 10% FBS for 3 hours. Following blocking, the wells were washed three times for 5 minutes with 400 µL PBST. The wells were then probed with 150 µL of concentrated medium (10X) containing one of the fusion proteins at 4ºC overnight. The following morning, the wells were washed three times for 5 minutes with 400 µL PBST. Wells probed with medium containing a fusion protein were probed with a rabbit anti-murine tissue factor polyclonal antibody (American Diagnostica, Stamford, CT) and control wells were probed with a rabbit anti-CEA polyclonal antibody (Abcam, Cambridge, MA) at serial dilutions overnight at 4ºC. Following incubation, the wells were washed three times for 5 minutes with 400 µL PBST. The wells were then probed with a goat anti-rabbit HRP-conjugated secondary antibody (Abcam, Cambridge, MA) for 1 hour at 37ºC. Wells were washed ten times for 5 minutes with 400 µL PBST. HRP activity was initiated by addition of 150 µL of undiluted 2, 2'-azinobis [3-ethylbenzothiazoline-6-sulfonic acid] - diammonium salt (ABTS) (Pierce, Rockford, IL) to each well for 30 minutes at room temperature. The reaction was quenched with the addition of 100 µL of 1% SDS. The plate was read at a wavelength of 405nm on a Molecular Devices plate reader and the results were captured using SoftMax Pro Software (Molecular Devices, Sunnyvale, CA).

CEA binding by immunofluorescence

5 X 10^5 HT-29 cells were seeded on polylysine coated glass slips inside 12 well plates overnight. The following morning the media was removed from each well and the wells were washed 3 times for 5 minutes with PBS. The cells were then fixed to the glass slips with 4% formalin in media for 10 minutes. The wells were then washed 3 times for 5 minutes each with PBS. Positive control wells were incubated with a polyclonal antibody to CEA (Abcam,

Cambridge, MA) at a dilution of 1:100. Negative control wells were incubated with a rabbit anti-murine tissue factor polyclonal antibody (American Diagnostica, Stamford, CT) at a dilution of 1:100 and the remaining wells were probed with media from 293T cells transiently transfected with the plasmid pMSZ/CBA-anti-CEA/tTF. Wells probed with the transfected media were detected with the rabbit anti-murine tissue factor polyclonal antibody (American Diagnostica, Stamford, CT) at a dilution of 1:100 and all wells were illuminated with an Alexa Fluor 594 conjugated donkey anti-rabbit antibody at a dilution of 1:500. The glass slips were removed from the wells and placed upon glass microslides with droplets of Vectashield with DAPI (Vector Labs, Burlingame, CA). The results of the immunofluorescence staining were evaluated on a Leica DM2500 fluorescent microscope (Leica Microsystems Inc, Bannockburn, IL) with an Optronics Camera Magnifier Software (Optronics, Goleta, CA).

Anti-TEM8/tTF Binding

The binding specificity of the anti-TEM8 fusion protein was shown via Western blotting. Briefly, 10 cm tissue culture plates (Thermo Fisher Scientific, Rochester, NY) containing 4.5 x 10^6 293T cells were transiently transfected with Sleeping Beauty vectors expressing one of three fusion proteins using calcium phosphate precipitation. The plates were incubated 72 hours post-transfection. Medium from these plates were passed through a 0.2 μm filter and concentrated using Amicon® 30 cartridges (Millipore, Billerica, MA). The concentrated medium from each group was used to probe a separate PVDF membrane containing 30 μg of cell lysate from either 293T/TEM8 or 293T/CMG2 in adjacent lanes. Binding by the fusion proteins was detected using a rabbit anti-mouse tissue factor antibody followed by a goat anti-rabbit HRP-conjugated secondary antibody (Abcam, Cambridge, MA). The parental monoclonal antibody, SB5, concurrently probed another blot with the same cell lysates. A goat anti-mouse HRP-conjugated secondary antibody (Abcam, Cambridge, MA) was used for detection in this blot.

Tissue Factor Activity of the Fusion Proteins

Murine tissue factor activity was demonstrated by using purified protein components of the extrinsic pathway of blood coagulation available from R&D Systems (Minneapolis, MN). Briefly, 10 cm plates containing 293T cells were transiently transfected with pMSZ/CBA-anti-TEM8/tTF, -anti-CEA/tTF or -Dead-sc/tTF using calcium phosphate precipitation. Medium from each plate was collected 72 hours post transfection and passed through a 0.2 μm filter. The samples were then purified using nickel column chromatography except the samples were eluted in a total volume of 3.5mL and passed through a PD-10 desalting column (GE Healthcare, Uppsala Sweden) to exchange their buffer to 50mM Tris, pH 9.0. Fusion protein tissue factor activity was then analyzed using the R&D Systems (R&D Systems, Minneapolis, MN) murine tissue factor assay. Briefly, lyophilized recombinant murine factor VII (rmFVII, R&D Systems, Minneapolis, MN), recombinant murine tissue factor (rmTF, R&D Systems, Minneapolis, MN), thermolysin (R&D Systems, Minneapolis, MN) and fluorogenic substrate (R&D Systems, Minneapolis, MN) were reconstituted according to manufacturer's specifications. Thermolysin and rmFVII were incubated together 1:1 for 30 minutes at 37°C. The reaction was stopped by addition a 40mM 1,10- phenanthroline and additional incubation at 37°C for 5 minutes. Next, either a determined amount of control rmTF is resuspended in 37 μL of 50mM Tris, pH 9.0 or 37 μL of the nickel column purified fusion protein from the transiently transfected cells were incubated with 13.3 μL of the thermolysin processed rmFVII for 5 minutes at 37°C. Finally, 50 μL of 200 μM fluorogenic substrate was added to the reaction, and the reactions were read using the kinetic setting on a plate reader at excitation and emission wavelengths of 380nm and 460nm, respectively, for 5 minutes.

Animal Studies

All animal experiments were conducted with seven-week-old athymic nude mice purchased from Jackson Laboratory (Bar Harbor, ME) and were maintained under standard specific pathogen-free conditions. All procedures performed on the mice were reviewed and approved by the University of Florida Institutional Animal Care and Use Committee. In the tumor growth studies, mice received intramuscular injections of 1×10^6 HT-29 human colorectal carcinoma cells in the left hind limb region near the calf muscle in a total volume of 25 μL consisting of a 1:1 ratio of sterile phosphate buffered saline and matrigel (Becton Dickinson, Franklin Lakes, NJ). The mice were anesthetized with vaporized isoflurane and placed in the right lateral decubitis position. One-half milliliter tuberculin syringes with 30-gauge needles were used to inject the HT-29 cell suspension into the left calf of the mice in between the area where the tibia and fibula would meet with the tarsal. The needle was quickly inserted into this area about 5mm deep, and the 25 μl HT-29 cell suspension was injected. On days 7, 14, 21 and 28 post tumor injections, the mice received therapy which consisted of either no injection (untreated control) or a tail vein injection of 200 μL that consisted of a 5:1 molar ratio of a transposon plasmid that expressed a fusion protein and the Sleeping Beauty transposase expression plasmid (pCMV-SB16) that was complexed with the linear polymer polyethylenimine (PEI) (Polyplus Transfection, Illkirch, France) as per manufacturer's instructions. The mice were sacrificed at Day 30, and their tumor and lung tissue was harvested for immunohistochemistry and Western blot analysis.

The tumor growth delay studies were carried out using the same protocol as the tumor growth studies except animals received weekly injections of therapy until their tumor surpassed a volume of 1.3 cm^3. Once the tumors passed this endpoint, they were sacrificed and their tissue was harvested for immunohistochemistry and Western blot analysis.

Blood Concentration of the Anti-TEM8/tTF Fusion Protein

Circulating fusion protein levels in mice were determined using the same protocol as the tumor growth studies except animals were not given a tumor burden. Instead, animals were injected with the Sleeping Beauty vector pMSZ/CBA-anti-TEM8/tTF and pCMV-SB16 on days 7 and 14. Control animals received no injection. Peak circulating expression levels were determined by collecting blood on Days 0, 10 and 17 using a BD Microtainer (Becton Dickinson, Franklin Lakes, NJ) containing 25 µL 4% Na citrate by puncturing the facial vein with a Golden Rod Animal Lancet (Medipoint, Inc Mineoia, NY) while animals were under isoflurane anesthesia. The blood was analyzed using a capture ELISA assay. Briefly, wells of a Maxisorp 96-well plate were coated overnight at 4°C with 100 µL of a 5 µg/ml anti-His antibody in coating solution (0.2M Na bicarbonate pH 9.6). The wells were washed three times for 5 minutes with 400 µL PBST. Each well was then blocked with 200 µL of PBST + 10% FBS for 3 hours. Following blocking, the wells were washed three times for 5 minutes with 400 µL PBST. Next, the wells were incubated overnight at 4°C with either 150 µL of plasma from injected or non-injected animals or a serially diluted sample of a C-terminal His tagged recombinant murine tissue factor (R&D Systems, Minneapolis, MN) in PBST. The wells were then washed three times for 5 minutes with 400 µL PBST. Wells were probed with a rabbit anti-murine tissue factor polyclonal antibody (American Diagnostica, Stamford, CT) overnight at 4°C. Following incubation, the wells were washed three times for 5 minutes with 400 µL PBST. The wells were then probed with a goat anti-rabbit HRP-conjugated secondary antibody (Abcam, Cambridge, MA) for 1 hour at 37ºC. Wells were then washed ten times for 5 minutes with 400 µL PBST. Detection was initiated using 150 µL of ABTS (Pierce, Rockford, IL) to each well for 30 minutes at room temperature. The reaction was quenched with the addition of 100 µL of 1%

SDS. The plate was read at a wavelength of 405nm on a Molecular Devices plate reader and the results were captured using Software Pro Software (Molecular Devices, Sunnyvale, CA).

Immunohistochemistry

Tumors were dissected from the left leg of each mouse and immediately placed in 4% paraformaldehyde overnight. The samples were paraffin embedded and cut into 5 μm sections. After an overnight drying period, slides were deparaffinized and rehydrated to undergo either immunofluorescent analysis or H&E staining. Samples undergoing immunofluorescent analysis underwent one of three standard retrieval processes that were compatible with the primary antibodies. Studies utilizing the anti-CEA (Abcam, Cambridge, MA) and anti-CD31 (Santa Cruz Biotechnology Inc, Santa Cruz, CA) antibodies underwent a Proteinase K (Dako, Glostrup, Denmark) digestion for 2 minutes. Immunofluorescent staining with anti-TEM8 (Abcam, Cambridge, MA) and anti-MECA32 (Pharmingen, Becton Dickinson, Franklin Lakes, NJ; MECA32 is also known as murine plasmalemma vesicle protein 1) underwent a 20 minute incubation at 95°C with Target Retrieval Solution (Dako, Glostrup, Denmark) followed by a 20 minute incubation at room temperature in the same solution. Immunofluorescent staining with anti-TEM8 (Abcam, Cambridge, MA), anti-murine tissue factor (American Diagnostica, Stamford, CT), pentaHis 488 (Qiagen, Valencia, CA) and anti-CD34 (Abcam, Cambridge, MA) underwent a 0.01M Citra pH 6.0 retrieval for 25 minutes at 98°C followed by a cool time of 20 minutes at room temperature. All samples were washed with Tris-Buffered Saline (TBS) and blocked with normal horse serum (Vector Laboratories, Berlingame, CA) for 20 minutes at room temperature. Antibodies were diluted in antibody diluent (Zymed Laboratories, San Francisco, CA) and incubated on slides overnight at 4°C. The concentrations for the primary antibodies were as follow: Anti-TEM8 (1:75), anti-CD34 (1:100), anti-MECA32 (1:10), anti-murine tissue factor (1:100), anti-CEA (1:100), anti-CD31 (1:50), and pentaHis 488 (1:100). The slides were

then washed 3 times with TBS for 5 minutes and the secondary antibodies used were AlexaFluor donkey anti-rabbit 488 (Invitrogen Corporation, Carlsbad, CA) for anti-TEM8, anti-CEA and anti-murine tissue factor; and AlexaFluor donkey anti-rat 594 (Invitrogen Corporation, Carlsbad, CA) for anti-CD34, anti-MECA32, and anti-CD31. PentaHis 488 is primary conjugated and was not detected with a secondary antibody. The results of the immunofluorescent staining were evaluated on either a Leica DM2500 fluorescent microscope (Leica Microsystems Inc, Bannockburn, IL) with an Optronics Camera and Magnifier Software (Optronics, Goleta, CA) or an Olympus 1X81-DSU spinning disk confocal microscope with Slidebook software (Olympus, Center Valley, PA).

Tumor Microenvironment Assessment

Quantifying Tumor Vessel Density

To assess and quantify the vessel density of tumors in the xenograft model, section slides were stained with the anti-Meca32 antibody. First, a 100x magnification was used to scan slides to find highly vascular areas in four separate regions per slide. Then, a 200x magnification was used to quantitate the areas with the greatest amount of vascular density and the average of the four areas was collected per slide. Areas positive for Meca32 that were distinct from other areas positive for Meca32 were considered a separate microvessel and counted as such.

Evaluating Tumor Vessel Thrombosis

Visualization of localized thrombosis events in the tumors was evaluated at two points. The first point was at tissue collection when tumor samples were portioned into thirds to ensure proper fixation. At this time point, thrombosis events could be visualized with the unaided eye for anti-CEA and anti-TEM8 treated animals. The second point occurred following H&E staining when samples were examined by microscopy at 50x, 100x and 200x magnification. Thrombosis events were only considered genuine if the area was surrounded by large areas of

necrosis marked by fragmentation of the tissue. In addition, areas along the outer one third portion of the tumor were only considered for thrombosis events since necrosis is widely reported in the center of xenografted tumors.

Western Blot Analysis of Tumor and Lung Tissue

After resection, murine lung and tumor tissue was cut up into smaller pieces and washed in sterile phosphate-buffered saline, pH 7.4. The tissue was centrifuged and resuspended into sample application buffer containing a protease inhibitor cocktail (Roche, Indianapolis, IN). The samples were homogenized using a Dounce Homogenizer cooled to 4°C and incubated overnight at 4°C on a rotary shaker. The next day the tissue was passed through a 30 gauge needle. The resulting lysate was then cleared via centrifugation at 10,000g for 10 minutes at 4°C. The supernatant was collected, boiled at 100°C for 5 minutes and 100 μg was run on an 10% SDS-PAGE gel that was transferred to a PVDF membrane and blotted against a murine primary HRP-conjugated anti-His monoclonal antibody against (Invitrogen Corporation, Carlsbad, CA).

PVDF Membrane Stripping and Actin Blot for Equal Loading

Blots were stripped by incubation at 50°C with stripping buffer (62.5mM Tris-HCl pH 6.8, 2% SDS, 5% beta mercaptoethanol) for 30 minutes and washed with 2x with PBST. To show equal loading, the blots were reblocked overnight with milk buffer and probed with an anti-actin antibody (Abcam, Cambridge, MA) for 2 hours at room temperature followed by 3 washes with PBST and a goat anti-mouse HRP conjugated secondary antibody (Abcam, Cambridge, MA).

Statistical Analysis

Data collected was analyzed using GraphPad Prism software (La Jolla, CA). Comparisons between the means of each group were analyzed using one-way analysis of variation. For the tumor growth study, a two-way analysis of variation was used when the mean tumor growth between each of the treatment groups were compared followed by a Bonferroni post test to

compare individual time points between each of the groups. For the tumor growth delay studies, data were analyzed using a Kaplan Meier curve and the mean survival for each group was compared using a Log Rank test. Data were shown as mean with standard error of measurement. All statistical tests were two sided and the threshold for statistical significance was $p < 0.05$.

CHAPTER 3[1]
SLEEPING BEAUTY

Introduction

Sleeping Beauty is a member of the Tc1/*mariner* superfamily of DNA transposons which are believed to be the largest family of transposons having members in a variety of species including fish, fungi, plants, humans and nematodes (53). All members of this superfamily share common characteristics, which are exemplified by similarities in their respective transposase proteins and their "cut-and-paste" method of transposition (53). Sleeping Beauty was synthetically resurrected by comparing fossil transposon elements from several species of salmonid fish to create a consensus sequence from one that was dormant for approximately 10 million years (54); hence, its name (55).

Since its revival, Sleeping Beauty has been employed for two main purposes within basic research: gene delivery and gene discovery. As a gene delivery vehicle, Sleeping Beauty has successfully undergone transposition in numerous cells and primary tissues including cell lines (56-59); zebrafish embryos (60-62); murine embryos (63); murine germ cells (64-68); murine stem cells (69), nonhematopoietic stem cells (70); murine somatic tissue (71-79), human primary blood lymphocytes (80) and human embryonic stem cells(81). For gene discovery, Sleeping Beauty has been used as an insertional mutagenesis tool to identify cancer genes utilizing a forward genetic screen (63, 66, 82). Both applications of Sleeping Beauty have yielded interesting data illustrating the utility of this genetic element.

Similar to other members of the Tc1/*mariner* family, the structure of Sleeping Beauty is simple and consists of two components: the transposon and the transposase (55). The transposon

[1] Text and figures in this chapter were modified from the publication: Fernando S, Fletcher BS. Sleeping beauty transposon-mediated nonviral gene therapy. BioDrugs 2006;20(4):219-29.

is the DNA surrounded by the two terminal inverted repeat/direct repeat elements (IR/DRs) (55). The transposase is the protein that facilitates the act of transposition by binding to the DR regions within the IR/DR elements (55). Together, these two components act in a "cut and paste" manner to move the transposon in its entirety from the donor plasmid or location to a TA dinucleotide within the recipient piece of DNA (55, 79). In its native state, the gene for Sleeping Beauty transposase resides within the IR/DR regions (55). This property gave that transposon the ability to hop around the genome at random and likely contributed to genetic diversity. As a gene therapy vector, this attribute would be undesirable, therefore, the system has been resolved into two components: the transposon, which is flanked by IR/DR elements and contains an internal promoter to drive expression of a gene of interest, and the transposase, which is expressed in either a cis or trans configuration. A schematic representation of the transposon and transposase provided in the *trans* configuration is depicted in Figure 3-1.

Structure of the Sleeping Beauty Transposon

The two terminal IR/DR elements flanking the transposon consist of ~230 base pairs (bp) containing two 30bp direct repeats separated by 170 nucleotides (Figure 3-1B) (55, 83, 84). Each IR/DR is distinguished as either the "left" or "right" and the DR elements where the transposase binds are further classified as either "inner" or "outer" (83, 84). Importantly for gene therapy, the human genome does not harbor any elements that directly resemble the Sleeping Beauty IR/DR elements. Further analysis reveals the four DR elements are not identical in sequence, but contain subtle differences that have an impact on transposition efficiency. Elegant experiments have examined the importance of the DR elements sequence composition, spacing, size constraints and the ability to substitute for one another (83, 84). These results suggested that the placement, order and sequence of the DR elements are essential for proper function.

With the knowledge obtained regarding the essential *cis*-acting elements within the transposon, improvements were made with the goal of enhancing transposition efficiency. The areas most extensively examined included the transposon sequence, the sequence flanking the transposon and the distances separating the IR/DR elements. Site directed mutagenesis to the right IR/DR element, as well as the addition of TA dinucleotides to the outside ends of the transposon, improved transposition several fold (83). Manipulation of the distances separating the IR/DR elements further provided information about the size constraints of the system (57, 59, 73, 85). Shortening of the distance outside of the IR/DR elements enhanced transposition by about two fold (59). Increasing the size of DNA within the transposon negatively affected transposition with ~15% loss of transposition activity for each kilobase (kb) beyond 2 kb (57). This carrying capacity is large enough to deliver the majority (~80%) of human cDNAs (86) and with a novel sandwich transposon design, is capable of carrying even larger payloads (87). Based upon these results, improved transposon vectors for gene therapy were developed including the pT2/ (83), pT3/ (88), pMSZ/ (73) and pT/SA vectors (89). In addition to delivering therapeutic genes, expression cassettes encoding short hairpin RNAs could also be used to downregulate specific gene products (58, 90, 91).

The Sleeping Beauty Transposase

The Sleeping Beauty transposase contains several domains that are conserved amongst several different transposon families. These include an N-terminal paired-like DNA-binding domain, a nuclear localization signal and a C-terminal integrase domain containing the essential DD(35)E motif (55). The DD(35)E motif is an evolutionarily conserved region found not only within the Tc*1*/*mariner* family, but also within eukaryotic retrotransposons, prokaryotic transposases, and retroviral integrases (55, 92, 93). This domain catalyzes the excision and insertion of the Sleeping Beauty transposon (94, 95). Once these domains were recognized, it

allowed researchers to manipulate the sequence of the original transposase in order to generate hyperactive mutants.

SB10 is the original reconstructed Sleeping Beauty transposase, which was able to achieve transposition frequencies of approximately 0.3% when delivered to HeLa cells (55). This result is 20-40 times more efficient than random integration, however the transposition efficiency can vary and is highly dependent on the cell line transfected as other cell types give lower levels of transposition (56, 59). While these results were encouraging, there was still considerable room for improvement if the vectors were to be used for gene therapy purposes. To date, at least four separate attempts have been made to create transposase mutants with increased transposition activity. The strategies employed include phylogenetic comparisons of related transposons (57, 96), rational mutagenesis by extrapolating mutations from other hyperactive transposases (89), and alanine scanning mutagenesis (88). From these studies, it appears that certain combinations of hyperactive mutations can have synergistic activities, while other combinations are detrimental. With these changes, transposition efficiencies have significantly increased yielding vector systems that can now be effectively applied to *in vivo* gene therapy.

In addition to the transposase, several cellular factors have recently been identified that may facilitate the transposition process. The DNA-bending, high-mobility group protein, HMGB1, was the first host factor found to enhance transposition (87). Additional studies have shown the importance of factors that mediate nonhomologous end joining (NHEJ), including the catalytic subunit of the DNA-dependent protein kinase (94). Finally, Sleeping Beauty transposase has recently been found to associate with the transcriptional factor Miz-1 (Myc-interacting zinc finger protein) (97). The association between the two proteins causes a brief G1 arrest that is believed to enhance the transposition efficiency of Sleeping Beauty (97). This

interaction, as well as other results, suggests that Sleeping Beauty may prefer to mobilize in the G1 stage of the cell cycle (97). The identification of host proteins that facilitate transposition could have an important impact on the use of Sleeping Beauty in gene therapy, as transient expression of those proteins could markedly enhance the poor transposition rates seen in certain cell types.

Basic Mechanism of Transposition

Sleeping Beauty transposition proceeds by a series of successive steps, in which the transposon is cut from the donor location and integrated into the target TA dinucleotide (Figure 3-1C and Figure 3-2) (55). The first step in transposition is the binding of transposase to each DR element forming a tetrameric protein/DNA complex (83, 84, 88). The two ends of the transposon are brought together by interactions between the bound transposase molecules forming the synaptic complex. Synaptic complex formation is a prerequisite for the completion of subsequent steps of transposition and is potentially facilitated by the host factor HMGB1 (87). The reaction proceeds by excision of the transposon from the donor location by specific staggered DNA breaks at each end of the transposon creating 3' overhangs (66, 94, 98). The 3` hydroxyl on each side of the transposon invades the target TA dinucleotide on the recipient DNA strand via nucleophilic attack. This results in two single-strand gaps of five base pairs in length that flank the unrepaired integration intermediate. The gaps are filled in by host factors that have yet to be clearly identified. These events duplicate the original target TA dinucleotide, leaving one "TA" on each side of the transposon (94, 98). The donor plasmid is then repaired by nonhomologous end joining which leaves behind a distinguishing footprint at the site of excision (94, 98). This characteristic has led to the development of an "excision assay" that can be used to illustrate excision from a donor plasmid (99). Since excision does not always lead to transposition, the excision assay needs to be accompanied by a selectable or quantifiable marker

to differentiate transposition mediated by Sleeping Beauty transposase as opposed to non-transposition related integration. Although the fidelity of this process is usually very high, it is not absolute, as variations in footprints have been observed in certain cell lines and in cells deficient for double strand break repair factors (94, 98).

Lastly, DNA methylation of the transposon has been reported to play a role in Sleeping Beauty transposition (100). CpG methylation has been shown to increase the excision of the transposon from chromosomal and donor plasmid locations in mouse embryonic stem cells and mouse erythroleukemia cells, respectively (100). In addition, transposition from a donor plasmid to chromosomal DNA was enhanced 11 fold in mouse embryonic stem cells when comparing a methylated versus an unmethylated Sleeping Beauty transposon (100). These findings suggest DNA methylation plays an important role in regulating transposition leading the authors to hypothesize two models that might explain their findings. The first model, called the inhibitor model, states that methylation of the Sleeping Beauty transposon causes inhibitory host factors to dissociate away from the transposon (100). The second model, called the enhancer model, states that methylation of the Sleeping Beauty transposon enhances the transposase ability to bind the IR/DR regions (100). While neither model has been proven, it is important to note that similar methylation experiments conducted in our laboratory have resulted in only minor improvements in transposition within HeLa cells. Furthermore, even in the original report, methylation of a different transposon system, the Tc3 transposon, only produced a 2-fold increase in transposition (100). To further complicate the picture, CpG methylation is well known to cause transcription silencing of promoters (101). For the purposes of gene therapy, this consequence is undesirable even if the methylation enhances transposition efficiency. In order to make the methylation

enhancement work, solutions for overcoming the silencing of the promoter must be incorporated into the CpG methylated transposon vectors.

Target Site Selection

The Sleeping Beauty transposase facilitates integration into TA dinucleotides within the target DNA (55). While this preference is an inherent property of the transposase, other studies have suggested that certain physical properties within the target, such as AT-rich areas, DNA bendability or a palindromic pattern of hydrogen-bonding sites may influence target selection (102, 103). On a genome wide scale, the location of integration events was initially thought to be completely random, showing little or no preference for introns, exons, or regulatory sequences (64, 103). However, in a much larger study of 1,336 integration sites, a slight preference toward integration near transcriptional units was observed (104). While integration near transcriptional units has been a major safety concern for a number of the viral gene therapy vectors, including retroviral and HIV-1- based lentiviral vectors, Sleeping Beauty appears to have the lowest frequency of intragenic integrations making it the safest integrating vector system to date (104). No chromosomal abnormalities were observed surrounding the target integration site, other than the duplication of the target TA dinucleotide. Furthermore, recent attempts at targeted transposition have yielded encouraging results (105). This information is valuable for future assessment of the risks associated with using Sleeping Beauty in human gene therapy trials.

Delivery of the Sleeping Beauty Transposon Components

For the Sleeping Beauty transposon to be effectively used in gene therapy, both components of its system must be present concurrently within the target cell. Given this requirement, various approaches have been used to deliver the essential components. Because the transposon must be in the form of DNA, plasmids have been used most often to deliver this component. Currently, pT2/ (83), pT3/ (88) and pMSZ/ (73) are the most active plasmids in

transposition assays. The transposase, on the other hand, is a protein and thus can be delivered in multiple ways in order to facilitate transposition which include: a purified protein, an mRNA encoding the transposase (106), a transposase expression plasmid (79), or a *cis*-plasmid which contains both the transposon and the transposase (107). Each of these approaches has been tested except the use of purified transposase. The only concern with the delivery of transposase is that high levels of expression can actually lead to reduced transposition: A phenomenon termed overproduction inhibition, which is observed for several other transposable elements (108). Therefore, when using two separate plasmids to deliver the transposon and transposase, the molar ratios of these plasmids are optimized to enhance transposition (range of 3:1 to 25:1 transposon to transposase, depending on the target tissues). In the *cis*-plasmid system, the strength of the promoter driving the transposase needs to be reduced in order to enhance transposition efficiency (107). The molecular details that regulate overproduction inhibition are unclear, but may involve extra transposase molecules not associated with the synaptic complex interfering with integration or excision.

In Vivo Delivery of Sleeping Beauty

Once the vectors for Sleeping Beauty transposition have been chosen, a method for delivery must be considered. One advantage viruses have over nonviral vectors is the ability to package their transgene payload into a capsid for delivery. In contrast, nonviral vectors are delivered as naked plasmid or utilize various chemical agents to form deliverable complexes. A number of different complexes have been made including lipoplexes (cationic lipid/DNA complexes) (109), polyplexes (cationic polymer/DNA complexes) (110) and lipopolyplexes (lipid and polymer/DNA complexes) (110). Other approaches include artificial viruses (like the HVJ) (111), and various physical methods such as hydrodynamic therapy (112), extravasation therapy (113), electroporation (114, 115) and gene guns (116). In addition to these techniques,

efforts have been made to create hybrid Sleeping Beauty /viral vectors that take advantage of the high transduction efficiencies of some non-integrating viruses such as adenovirus and herpes simplex virus and combine them with integrating ability of Sleeping Beauty (78, 117). Of these available methods, the two techniques employed most often for the *in vivo* delivery of Sleeping Beauty transposons are hydrodynamic therapy (118) and polyplex complexes (119) using the linear polymer polyethylenimine.

Hydrodynamic Therapy

Hydrodynamic therapy is based on the principle that the physical barriers protecting parenchymal cells from unwanted invasion can be overcome by briefly increasing lumenal pressures to promote extravasation. This principle allows naked genetic material to be delivered via high volume/pressure injection without the need for additional chemicals or formulations. When high volume naked nucleic acid injections were given to mice via the tail vein, high-level transfection of hepatocytes was observed up to 40% (120). Modifications of this technique to target tissues other than the liver have also been developed (121). Adverse effects due to the pressure required to penetrate the endothelium and parenchymal cells have been observed and include cellular destruction (122, 123), angiopathy (124) and organism death (125). However, these negative side effects can be managed by control of hydrodynamic parameters such as the volume of injection and speed of delivery (122, 124). This observation is supported by recent studies in mice and larger vertebrates that resulted in transfection without angiopathy or organism death (121). Therefore, this technique holds promise as a way to deliver therapeutic plasmids to various tissues.

Yant et al., was the first to use the hydrodynamic approach to deliver plasmids encoding the Sleeping Beauty transposon system (79). This group showed that without Sleeping Beauty transposase or the IR/DR elements, expression of the reporter genes was lost with time with

random integration occurring in ~0.01% of hepatocytes, yet with the elements long-term expression was observed in 2-3% of hepatocytes. Using a murine hemophilia B model, they were able to achieve therapeutic levels of FIX resulting in phenotypic correction of the bleeding disorder. Since then, several other groups have used hydrodynamic therapy to deliver therapeutic genes to the liver including insulin, the FAH gene, and FVIII (Table 3-1).

Polyplexes Composed of Polyethylenimine (PEI)

Formulation of nucleic acids with cationic lipids or polymers can enhance transfection efficiencies both *in vitro* and *in vivo*. The exact mechanism by which these agents facilitate the cellular uptake and intracellular trafficking of DNA to the nucleus remains an area of intense interest (126). Polyethylenimine is one of the most efficient agents at promoting transfection and is routinely used because of its commercial availability and ease of use (127). Complex formation is simple as electrostatic charge interactions between the polymer (nitrogen) and DNA (phosphate) promote polyplex self-assembly. The complex formed has a neutral center and a cationic surface that facilitates cell binding (128) likely through a group of transmembrane adhesion molecules called syndecans (129). Once inside the cell, PEI is still thought to confer benefits to the complexed DNA by protecting it from lysosomal degradation and cytoplasmic nucleases (128, 130).

Polyethylenimine shows further promise as it can be used *in vivo* with minimal toxicity. Systemic delivery of PEI/DNA complexes via injection tends to transfect endothelial and parenchymal cells within the first capillary bed it reaches; in the case of intravenous injection, lung transfection predominates (131, 132). Polyethylenimine has also been used to target the lung by other approaches including intra-tracheal instillation (133) or inhalation of aerosols (134). To target certain tissues more specifically, direct intra-arterial or intra-parenchymal injections have been performed within the kidney (135), brain (136) or into tumors (137).

Toxicity associated with the use of PEI has been minimal, however endothelial cell dysfunction was observed (138) and animal death will occur if administered systemically at high concentrations.

Several laboratories have used PEI to deliver Sleeping Beauty transposons targeting certain tissues (Table 3-1). Systemic administration via intravenous injection mainly targets lung tissue and pneumocytes as expected (71). The use of a cell-type specific promoter (endothelin-1) within the transposon was able to facilitate expression within endothelial cells (73). In both of these cases, long-term expression was observed compared to animals receiving non-functional transposase. Systemic administration of an endothelial-targeted transposon within neonatal mice was also able to direct expression of the FVIII gene within endothelial cells of the lung. Therapeutic levels of FVIII expression continued for over 6 months providing phenotypic correction of the disorder (139). In another example, direct intra-tumoral injection of anti-angiogenic genes within a Sleeping Beauty transposon was able to promote tumor regression in a glioblastoma model (75). In addition, our laboratory has data on using PEI and Sleeping Beauty transposons to express the endothelial nitric oxide synthase (NOS3) gene to reduce pulmonary and systemic hypertension (unpublished results), as well as the use of the indoleamine 2,3-dioxygenase (INDO) gene to reduce lung transplant rejection (140). These examples illustrate the power of combining an efficient polyplex with the Sleeping Beauty transposon system for long-term expression.

Ex Vivo Gene Delivery of Sleeping Beauty

Ex vivo gene therapy encompasses the process of taking cells from an individual, altering them genetically outside of the body, and placing them back into the recipient to alleviate or treat a medical condition. The benefits of this approach include targeted therapy, the possibility of selection of transfected clones, and minimizing the risks of collateral transfections occurring

locally or systemically. Target tissues have included hematopoietic stem cells (80, 141), myoblasts (142, 143), keratinocytes (77, 144) and fibroblasts (145). Traditionally, retrovirus has been used to transfect cells outside of the body due to high transfection efficiencies and a well-established proof of concept. This approach was the gold standard until the therapy went to clinical trials for X-linked severe combined immunodeficiency and insertional mutagenesis caused leukemia in two of the ten patients (146). This event led to a brief termination of all trials using retroviral *ex vivo* gene delivery and strengthened the search for safer vector systems.

Ex vivo use of Sleeping Beauty has been applied to several different cell types including embryonic stem cells (69, 81), keratinocytes (77), multipotent adult progenitor cells (70) and terminally differentiated T cells (80, 147) (Table 3-1). Each approach has been successful showing long-term expression and reasonable transfection efficiencies. The ability to stably transfer genes into primary peripheral blood lymphocytes, could show promise in the treatment of cancer (148-151), viral infections (151, 152) and immunodeficiencies (153). Transfection, in this study, was demonstrated without the need for T-cell activation (80). This attribute is beneficial since T-cells can alter their phenotype when stimulated in culture by cytokines (154). It will allow for the cells to be used immediately *in vivo* without further expansion (80). These characteristics of *ex vivo* transfection of Sleeping Beauty into T-cells has many similarities to transduction using HIV-1-based lentiviral vectors, however, two important differences exist. First, HIV-1-based vectors integrate most often (80% of the time) into actively transcribed regions of the genome compared to Sleeping Beauty, which integrates near genes with a frequency of ~39% (104). This statistic implies that HIV-1-based vectors are two-fold more likely to cause insertional mutagenesis compared to Sleeping Beauty-based vectors. Second, HIV-1-based vectors achieve transduction efficiencies of up to 50% in T-cells (155), whereas

Sleeping Beauty was only able to achieve 11% stable transposition (80). Though this difference is great, narrowing of this gap may occur since these experiments did not use many of the recently described improvements that enhance Sleeping Beauty transposition.

Risk and Benefit of Transposon-Based Gene Therapy

Since its reawakening, Sleeping Beauty has established itself as a viable alternative to viral-based gene therapy. In this field, Sleeping Beauty is unique because it incorporates many of the desirable characteristics of both viral and nonviral systems, like its ability to carry large amounts of genetic material, its long-term gene expression and its easy, safe and scalable production protocol. The major caveats to the use of Sleeping Beauty are insertional mutagenesis and the possibility of immune responses to the naked DNA, the transposase protein or the therapeutic transgene.

Just like retrovirus and HIV-1-based lentivirus, Sleeping Beauty integrates into the genome. This aspect of transposition is a double-edged sword since integration on one hand endows the vector with the ability to achieve long-term expression, yet on the other hand, promotes the risk of insertional mutagenesis. The outcome depends both on the location of the insertion, as well as the nature of the inserted transposon. Using transgenic mice harboring transposons specifically designed to both disrupt and drive transcription at integration sites (pT2/Onc vectors), two groups showed that breeding the pT2/Onc transgenics to transgenic mice harboring constitutively expressed Sleeping Beauty transposase resulted in tumor formation (82, 156). However, for one of the groups, no tumors were observed in mice of wild type genetic background and the use of mice lacking the tumor suppressor gene p19*Arf* was required (82). Therefore, under certain situations, such as in the presence of constant transposase expression and a disruptive transposon, oncogenesis is possible. However, with the use of more traditional expression transposons commonly used in therapeutic gene therapy, no other evidence for

spontaneous tumorigenesis has been observed. Approaches to reduce the likelihood of Sleeping Beauty-based mutagenesis and tumor formation include the use of RNA or protein to deliver the transposase (106). This would eliminate the possibility of continued transposase expression that has been observed with systemic administration of a plasmid bearing the transposase (157). Furthermore, safer transposons containing insulator sequences have been developed (158, 159). Despite these concerns, analysis of the target preferences of Sleeping Beauty reveals it is still one of the safest integrating vector systems available (104). An ultimate solution to the problem of insertional mutagenesis may lie in targeted integration, a topic that is currently being explored (105, 160). While several groups are working on this problem, no system exists that has high efficiency and is completely specific.

Systemic injection of Sleeping Beauty has not been evaluated in a human clinical trial and thus the potential for unexpected immune responses still exist. Non-specific immune responses to naked DNA are well known and activate the innate immune response through the Toll-like receptors on leukocytes (161). Use of CpG methylated DNA can reduce this immune activation (162) and may even reduce immune responses to the transgene (163). The therapeutic transgene itself may also be recognized by the immune system as a foreign antigen, especially if the replaced gene is not expressed endogenously. For example, immune responses to the FVIII protein have limited the success of several gene therapy trials in mice and larger animals (164, 165). Immune responses to the transposase may be less problematic, as they may only limit the possibility of repeated applications. Before Sleeping Beauty is administered systemically in a clinical trial, studies should be performed to evaluate the immune responses to Sleeping Beauty upon single and multiple administrations in several animal models. Only when studies like these are completed can the immunogenic potential of Sleeping Beauty be discerned. As our past

experiences with gene therapy have taught us, unrecognized immune events can limit the effectiveness of therapy or even lead to fatal responses.

Despite these unanswered concerns, Sleeping Beauty will be used in its first clinical trial with human patients (166). The trial will evaluate the safety of using Sleeping Beauty to modify T-cells *ex vivo* to express a fusion protein that will aid in battling CD19+ B-lymphoid malignancies. The *ex vivo* approach alleviates some of the predicted obstacles the immune system may levy since systemic injection of the transposon DNA will not be necessary, but responses to the fusion protein are still possible. This undertaking is a huge first step for Sleeping Beauty research and the results are highly anticipated.

Conclusions

Sleeping Beauty has been investigated for just over a decade. In this time, Sleeping Beauty has proven itself capable of stable gene transfer into a number of vertebrate species and cell targets. To date, almost 200 references exist concerning Sleeping Beauty and the current trend suggests that increasingly more will be published each year. The only unfortunate aspect about all this research is that it has been difficult to compare results from the various laboratories as each are using different plasmid backbones, and unique versions of the transposase and transposon. If the goals are to fine-tune the vector system into something that can be used clinically, then standardization of the system components is needed and safety issues regarding insertional mutagenesis and potential immune responses must be thoroughly explored.

In addition to an improved and standardized Sleeping Beauty system, equally, if not more important is the development of clinically acceptable ways in which to deliver the components. While hydrodynamic therapy and PEI-based complex delivery have revolutionized the world of nonviral gene delivery in animal models, significant room for improvement still exists in the clinical arena. Generating more efficient formulations for *in vivo* transfection with less toxicity

and developing approaches for tissue or organ specific targeting are areas of significant interest. For instance, modification of the PEI polymer by the attachment of galactose residues increases targeting of hepatocytes (167). Also, the use of tissue-specific promoters to limit the expression of the transgene, the transposase, or both, may lead to better targeting of specific cells or tissues (73).

A final area of improvement for Sleeping Beauty system is to control where it integrates within the genome. Site-specific integration would be ideal for most clinical situations, however in life threatening disorders, such as cancer, the lack of target-site specificity becomes less critical. As stated earlier, Sleeping Beauty integrates exclusively into TA dinucleotides, which are abundant within the genome. The only proven factor that helps in selection of target TA dinucleotides is the physical properties of the surrounding DNA. Attempts to make the transposase more site-specific by attaching DNA binding domains at the N-terminus may influence target site selection, yet have impaired transposase activity (105, 168). As little is known about the three-dimensional structure of Sleeping Beauty, perhaps solving the crystal structure of the transposase bound to DNA would provide insight regarding the critical residues influencing target selection. Future generations of hyperactive transposase mutants might then provide higher specificity of target site selection and could overcome the problem of overproduction inhibition.

Table 3-1. Nonviral gene therapy applications of Sleeping Beauty

Approach	Transgene	Delivery Method	Animal Model or Cells Transfected	Reference
In vivo				
	Human FIX	Hydrodynamic injection	Haemophlia B-C57bl/6 mice	(79)
	FAH	Hydrodynamic injection	FAH-exon5 Mice	(74)
	Luciferase	PEI, hydrodynamic injection	C57Bl/6 mice, FVB/N mice, FVB/N SB-transposase – transgenic mice	(71)
	Insulin	Hydrodynamic injection	Induced diabetic ICR mice	(72)
	SEAP, GFP	PEI	C57Bl/6 SCID mice	(73)
	GFP, Neo Luciferase	PEI	BALB/c nude mice	(169)
	B-domain deleted FVIII	Hydrodynamic injection	Hemophilia A mice	(76)
	Statin-AE, sFlt-1	PEI	BALB/c nude mice glioblastoma	(75)
	B-domain deleted FVIII	PEI	Neonatal hemophilia A – mice	(139)
	IFN-γ	PEI	C57Bl/6 glioblastoma	(170)
Ex vivo				
	LAMB3	Polybrene shock	SCID mice	(77)
	DsRed, NGCD	Nucleofection	T cells	(80)
	DsRed, luciferase	Nucleofection	Immunodeficient mice	(70)
	CAR for CD19	Nucleofection	T cell	(147)
	GFP, firefly luciferase	Nucleofection	Human embryonic stem cell	(81)

DsRED = Discoma sp. red protein; FVIII = factor VIII; FIX = factor IX; FAH = fumarylacetoacetate hydrolase; GFP = green fluorescence protein; ICR = Institute of Cancer Research; INS = insulin; LAMB3 = laminin □3; MAPC = multipotent adult progenitor cells; ND = no data; NEO = neomycin resistance; NGCD =human nerve growth factor receptor/yeast cytosine deaminase fusion gene; PBL = peripheral blood lymphocytes; PEI = polyethylenimine; SCID = severe combined immunodeficiency; SEAP = secreted alkaline phosphatase protein; sFlt-1 = soluble FLT1 (fms-like tyrosine kinase 1); Statin-AE = murine angiostatin-endostatin fusion gene; IFN-γ = interferon gamma.

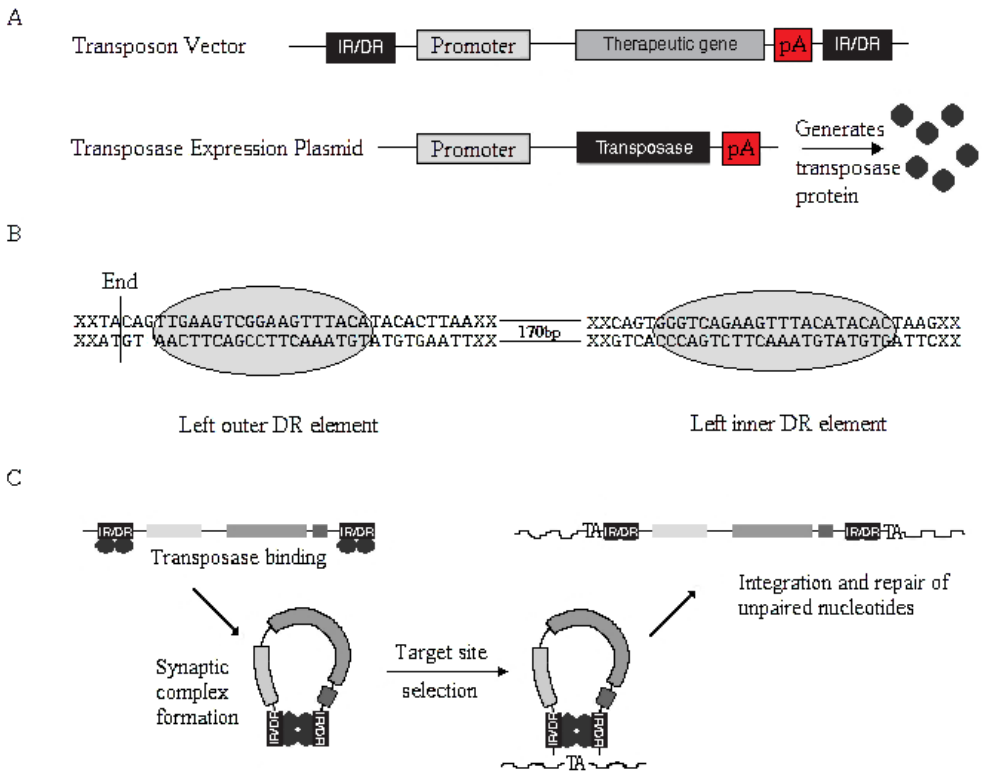

Figure 3-1. Diagram of the Sleeping Beauty vectors IR/DR elements and events in transposition. A) Typical donor plasmid used to carry the transposon and a typical transposase plasmid that would delivered in *trans*. B) Left IR/DR element with the area bound by the transposase highlighted in grey. C) The transposition event with the synaptic complex formation, excision of the transposon and insertion into the TA dinucleotide shown.

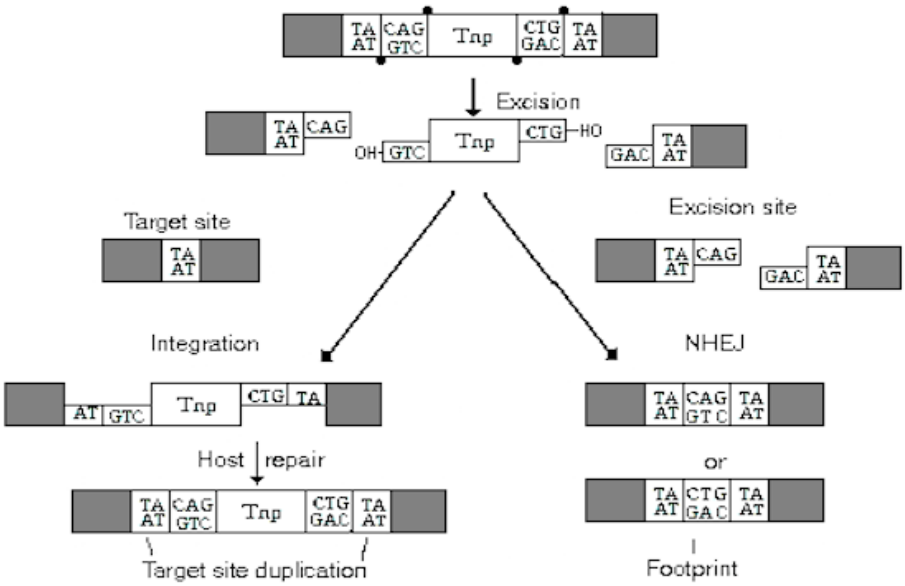

Figure 3-2. The transposition event. Transposase drives the excision and insertion of the transposon (Tnp) from the donor plasmid to the genomic DNA. Host repair enzymes repair correct single stranded gaps duplicating the target TA dinucleotide. Non-homologous repairs the excision site of the transposon from the donor plasmid.

CHAPTER 4
CONSTRUCTION OF THE FUSION PROTEINS AND *IN VITRO* ANALYSIS

Introduction

A fusion protein is a designed molecule that combines specific parts of protein domains and is encoded by a recombinant gene made via genetic engineering. Typically, these proteins have two active domains. The first domain allows for targeting of a specific ligand or receptor relevant to a disease. Examples of molecules used for targeting are small peptides, monoclonal antibody derivatives and interacting portions of proteins involved in the targeted pathway. The second domain mediates or enhances a pharmacological response and is commonly called an "effector domain." Common effector domains include cytokines, enzymes, toxins, and pieces or all of an antibody constant region. The use of fusion proteins in preclinical studies is common with many translating to clinical trials and few gaining FDA approval for clinical use (171). To complete this research, we created genes encoding fusion proteins that targeted the antigens TEM8 and CEA. The fusion protein genes are of similar design consisting of a scFv to target each antigen and truncated tissue factor to occlude tumor vasculature.

Single-Chain Antibodies

A single-chain antibody is a smaller derivative of a monoclonal antibody that retains only the variable light and heavy chains joined together by a peptide linker (47). These synthetic antibody constructs retain most of the specificity and affinity of the parent monoclonal antibody without the large constant regions attached (171, 172). This modification allows scFvs to penetrate tumors more efficiently and allows for quick elimination from the circulation through the kidney (171, 172). This characteristic may appear as a disadvantage when trying to home to a target, but this quality is beneficial since scFv and monoclonal antibodies raised against tumor antigens have endogenous human proteins as targets, which may be expressed in other areas of

the body. Thus, quick elimination of the antibody derivative serves as a protective measure against accidental collateral damage to areas of non-tumor associated antigen expression especially when scFv are used as the targeting domain of a fusion protein (171). Single-chain antibodies have a long history of being used as the targeting domain of fusion proteins and examples of antigens targeted by scFv include CEA (173), V-CAM (174), and the EBD domain of fibronectin (175).

Truncated Tissue Factor

Tissue factor is a membrane bound glycoprotein that functions as the initiator for the extrinsic pathway of blood coagulation (176). The first 219 amino acids of this protein act as a receptor for Factor VIIa (177) and are referred to as soluble or truncated tissue factor (tTF) when expressed recombinantly (48). The presence of this protein is privileged from areas that come into direct contact with the blood, and the closest tissue type known to express this protein in non-disease circumstances is the adventitia of blood vessels (178). The reason for this separation is simple: Tissue factor in the bloodstream is associated with endothelial or cellular wounds and the extrinsic pathway responds appropriately by clotting the blood in a fashion that seals the leak and restores hemostasis. The use of tTF in therapeutic models to occlude tumor vasculature is not new and is reported in at least three reports (174, 179, 180). In these reports, tTF is attached to either a ligand or a scFv directed against tumor antigens with the end result being the occlusion of the tumor vasculature. One caveat of this approach is the introduction of tTF to the main circulation with the fear being that systemic blood clot formation will occur, and thus, cause drastic thrombosis throughout the body. This fear, however, is put to rest with the knowledge that tTF is 10,000 times less effective than full length tissue factor (50, 179). The reason behind this difference rests with Factor Xa reliance upon phospholipids to become fully active (176). Accordingly, low levels of tTF floating in the bloodstream is not a threat to

activate the extrinsic pathway due to the lack of phospholipids, but as soon as tTF increases in concentration and becomes tethered to a cell, the threat becomes very real.

Fusion Protein Construction

Truncated Tissue Factor

RT-PCR on the mRNA from the brain tissue of a C57BL/6 mouse yielded a band of 695 base pairs (bp) which corresponded to the size of truncated tissue factor plus partial linker regions. We placed the PCR fragment into the shuttle vector pCR4 TOPO and sequenced the vector to ensure the fidelity of the sequence. We chose one clone with a correct sequence and modified the C-terminal domain by adding a mycHis tag via a PCR reaction. Sequence fidelity was verified and a correct sequence was chosen and set aside to construct the fusion proteins (Figure 4-1).

Anti-CEA/tTF Fusion Protein

RT-PCR on the mRNA from the HB-8747 hybridoma yielded a band of 446bp for the variable light chain and a band of 482bp for the variable heavy chain of T84.66 (Figure 4-2). These band sizes match the predicted size for each variable region plus the partial linker regions we added. The variable heavy chain was truncated by using primers that did not prime the secretion signal for amplification. Instead, we left the secretion signal on the variable light chain since a kappa light chain secretion signal is considered very strong. We placed the purified PCR fragments into the shuttle vector pCR4 TOPO and sequenced multiple fragments to find a correct clone. We chose one correct clone for each variable region and then proceeded to join the fragments together using SOE PCR. The results of the SOE PCR yielded a fragment of 908bp, which corresponded to the size of the T84.66 scFv plus a partial linker that would be used to join truncated tissue factor to the C-terminal end (Figure 4-3). Truncated tissue factor was added by an additional SOE PCR reaction to create the gene for anti-CEA/tTF. The gene was placed in

pCR4 TOPO and the sequence was verified to be correct. A single correct clone was ligated into the Sleeping Beauty expression plasmid pMSZ/CBA (Figure 4-4).

Anti-TEM8/tTF Fusion Protein

Separate 5`RACE reactions were performed for the variable light and heavy chains of SB5. The resulting bands were 635bp for the variable light chain and 490bp for the variable heavy chain. The PCR fragments for the each variable region was cloned into the shuttle vector pCR4 TOPO and sequenced. Since the DNA sequence for SB5 is not known we looked for areas such as secretion signals and open reading frames for assurance of sequence fidelity. To ensure we captured the correct sequence, we performed Q-STAR mass spectrometry on the SB5 monoclonal antibody to capture peptide sequences. We then compared those peptide sequences to the predicted amino acid sequences of the captured PCR fragments and found areas of alignment. We modified the sequences of the variable light and heavy chains to eliminate the constant regions amplified by the gene specific primers during 5`RACE and to add overlapping linker sequences via PCR reactions (Figure 4-5). We cloned the fragments into the shuttle vector pCR4 TOPO and verified sequence fidelity. As with the variable heavy chain region of T84.66, we eliminated the secretion signal on the variable heavy chain of SB5 through the PCR reactions. We then joined the variable light chain to the variable heavy chain via SOE PCR, which yielded a band of 813bp (Figure 4-6). The PCR fragment was placed in the shuttle vector pCR4 TOPO and sequenced. A correct clone was kept and labeled the SB5 scFv. Truncated tissue factor was added to the SB5 scFv by a subsequent SOE PCR reaction to form the gene for the anti-TEM8/tTF fusion protein. The gene was placed into the pCR4 TOPO vector and the sequence for this was gene was verified. One correct clone was ligated into the Sleeping Beauty expression plasmid pMSZ/CBA (Figure 4-7).

Dead-sc/tTF Fusion Protein

The variable light chain of the Dead-sc/tTF fusion protein was created by two separate PCR reactions on the variable light chain of SB5. The two PCR fragments were 167bp and 211bp. These fragments were placed inside the pCR4 TOPO shuttle vector and joined together by enzymatic digestion with *BglII* and *ScaI* followed by ligation of the fragments. The pCR4 clone with a fragment of proper size after ligation was sent for DNA sequencing to ensure the proper DNA sequences were removed. The variable heavy chain of the Dead-sc/tTF fusion protein was created by two separate PCR reactions on the variable heavy chain of anti-CEA/tTF. The two PCR fragments were 89bp and 957bp. These fragments were placed inside the pCR4 TOPO shuttle vector and joined together by enzymatic digestion with *XhoI* and *ScaI* followed by ligation of proper fragments. The pCR4 clone with a fragment of proper size after ligation was sent for DNA sequencing to ensure the proper DNA sequences were removed. The variable light chain of Dead-sc/tTF was joined to the variable heavy chain of Dead-sc/tTF with truncated tissue factor via SOE PCR since both fragments retained their partial linker region overlap. The resulting fragment was 1424bp. This fragment was placed into the pCR4 shuttle vector and sequenced. One correct clone was kept and labeled Dead-sc/tTF. The gene was placed into the Sleeping Beauty plasmid pMSZ/CBA (Figure 4-8).

In Vitro Analysis of the Fusion Proteins

Production and Secretion

Prior to initiating animal studies, we examined the expression vectors for their ability to produce functional fusion proteins in a cell culture system. To verify expression and secretion, 293T cells were transiently transfected with a transposon vector carrying the gene for one of the fusion proteins or the green fluorescent protein (GFP) as a control. After 48 hours, cell culture medium was collected and passed through nickel column chromatography. We examined the

eluted fusion proteins and crude cell lysates via Western blot analysis probing with an anti-6xHis antibody. Both blots yielded immunoreactive bands of ~65 kDa for the anti-TEM8/tTF protein, ~68 kDa for the anti-CEA/tTF protein and ~60 kDa for the Dead-sc/tTF protein (Figure 4-9). Crude cell lysates expressing GFP did not produce immunoreactive bands. These results are consistent with the predicted sizes for each fusion protein and confirm proper processing and secretion.

Binding Activity of the Fusion Proteins

To demonstrate the activity of our fusion proteins, we collected medium from the transient transfections to use in experiments. To demonstrate TEM8 binding activity, cell lysates from the cell lines 293T/TEM8 or 293T/CMG2 were run in adjacent lanes on an SDS-PAGE gel. Using Western blot analysis, the cell lysates were probed with the various fusion proteins or the SB5 monoclonal antibody (Figure 4-10). The SB5 monoclonal antibody and the anti-TEM8/tTF fusion protein detected a band of 42 kDa which corresponds to the predicted size of the over expressed TEM8 protein, while both proteins did not detect a band for the overexpressed CMG2 protein in the adjacent lane. Dead-sc/tTF, anti-CEA/tTF and control medium did not produce immunoreactive bands. To demonstrate the binding capability of the anti-CEA/tTF fusion protein, we utilized an ELISA assay using commercially available purified CEA protein (Figure 4-11). Dose dependent binding was observed with the anti-CEA/tTF protein, while Dead-sc/tTF and anti-TEM8/tTF did not bind. These results confirmed that the anti-TEM8 and anti-CEA single chain antibody domains retained their binding abilities. Dead-sc/tTF did not recognize either TEM8 or CEA in the same assays, confirming the predicted loss of affinity for either antigen.

Truncated Tissue Factor Activity

Activity of the tissue factor domains for each fusion protein was verified using an assay mimicking the activation of the extrinsic pathway of blood coagulation (Figure 4-12). For these experiments, all fusion proteins were purified from medium using nickel column chromatography due to fetal bovine serum and the dye in medium causing false positive reactions. The results from this assay showed that the truncated tissue factor domain from each fusion protein is active and yields quantifiable tissue factor activity when compared to a mock transfection, which had no activity. Together, these *in vitro* experiments showed that the fusion proteins are expressed, secreted, and maintained the predicted antigen recognition and tissue factor activity.

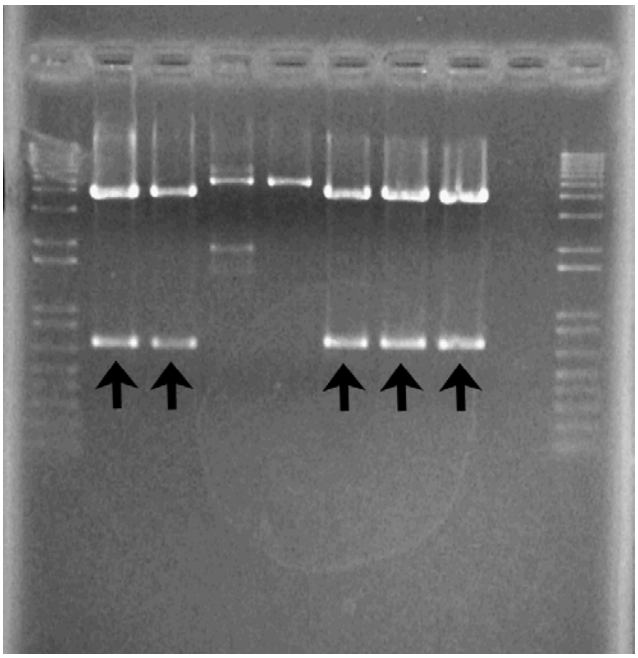

Figure 4-1.Truncated tissue factor. A PCR fragment containing truncated tissue factor with partial linker sequences was cloned into the vector pCR4 TOPO and cut out by *EcoRI* digestion. Arrows mark clones that contain a band of correct size. The DNA ladder shown is the standard 1 Kbp ladder.

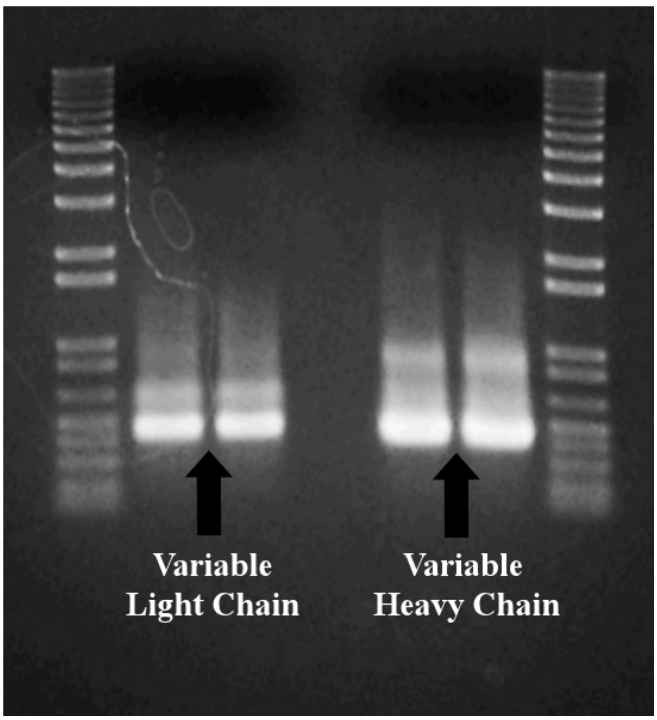

Figure 4-2. Variable light and heavy chain of T84.66. RT-PCR was performed on the mRNA from the HB-8747 hybridoma. The resulting bands (arrows) show the variable light chain was 446bp and the variable heavy chain was 482bp. The sizes of these bands are larger than the published sequences because of the addition of partial linker regions. The DNA ladder shown is the standard 1 Kbp ladder.

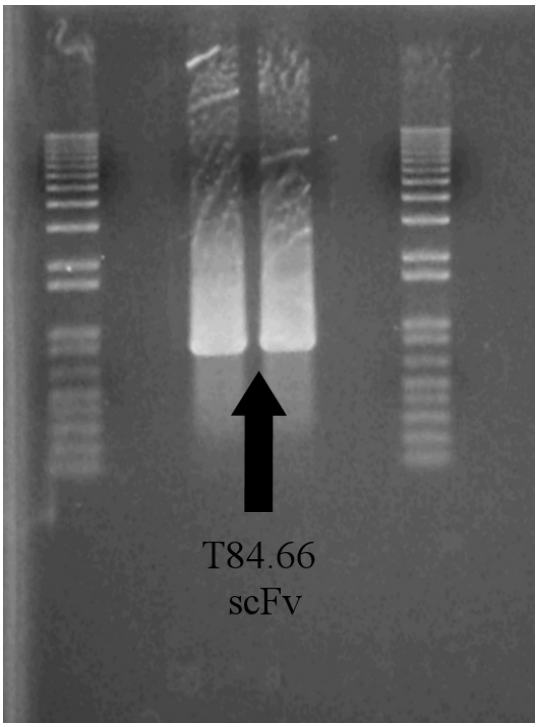

Figure 4-3. T84.66 scFv. The T84.66 scFv was formed by SOE PCR joining the variable light chain to the variable heavy chain. The PCR fragment is 908bp, which contains a partial linker region. The DNA ladder shown is the standard 1 Kbp ladder.

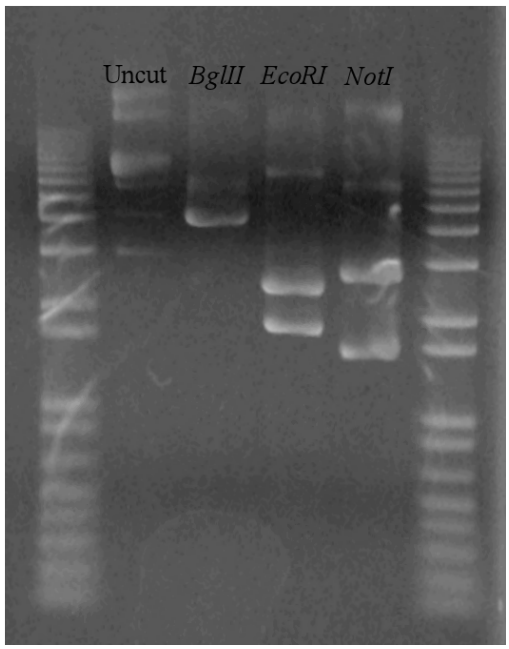

Figure 4-4. pMSZ/CBA-anti-CEA/tTF. The anti-CEA/tTF fusion protein gene was created by SOE PCR and placed into the expression vector pMSZ/CBA. The vector was characterized for purity, concatermerization, insertion, and orientation. Purity and concatermerization was checked by running uncut plasmid and linear plasmid (*BglII*) in adjacent lanes. Insertion was checked via *NotI* cut which released bands of sizes 2741bp and 1596bp. Orientation was checked by an *EcoRI* cut which released the correct band sizes of 2474bp and 1863bp. The DNA ladder shown is the standard 1 Kbp ladder.

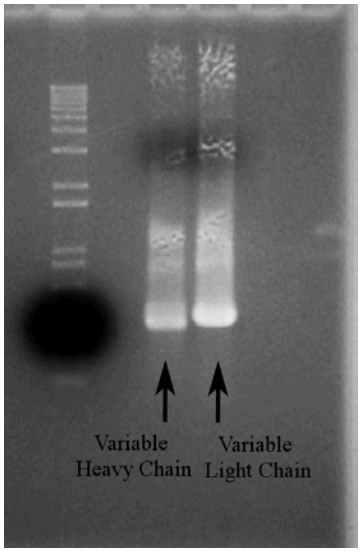

Figure 4-5. SB5 variable light and heavy chains. The variable light and heavy chain of SB5 was modified by a PCR reaction after the 5`RACE procedure to add partial linkers to both variable regions and eliminate areas amplified by the gene specific primers. The DNA ladder shown is the standard 1 Kbp ladder.

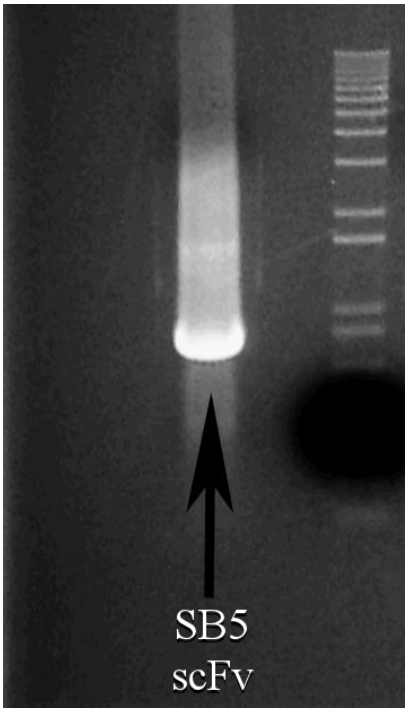

Figure 4-6. SB5 scFv. The SB5 scFv was formed by SOE PCR joining the variable light chain to the variable heavy chain. The PCR fragment is 813bp, which contains a partial linker region of the variable heavy chain. The DNA ladder shown is the standard 1 Kbp ladder.

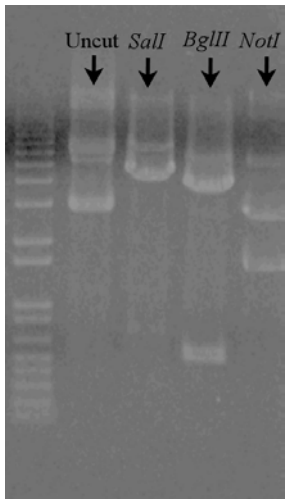

Figure 4-7. pMSZ/CBA-anti-TEM8/tTF. The anti-TEM8/tTF fusion protein gene was created by SOE PCR and placed into the expression vector pMSZ/CBA. The vector was characterized for purity, concatermerization, insertion, and orientation. Purity and concatermerization was checked by running uncut plasmid and linear plasmid (*SalI*) in adjacent lanes. Orientation was checked by a *BglII* cut which released the correct band sizes of 3783bp and 530bp. Insertion was checked via a *NotI* cut which released bands of sizes 2741bp and 1572bp. The DNA ladder shown is the standard 1 Kbp ladder.

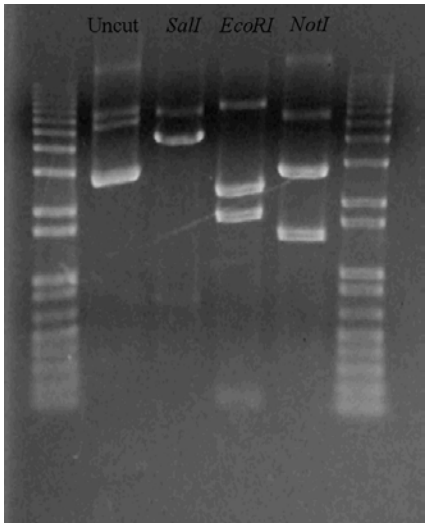

Figure 4-8. pMSZ/CBA-Dead-sc/tTF. The Dead-sc/tTF fusion protein gene was created by SOE PCR and placed into the expression vector pMSZ/CBA. The vector was characterized for purity, concatermerization, insertion, and orientation. Purity and concatermerization was checked by running uncut plasmid and linear plasmid (*SalI*) in adjacent lanes. Insertion was checked via a *NotI* cut which released bands of sizes 2741bp and 1413bp. Orientation was checked by a *EcoRI* cut which released the correct band sizes of 2294bp and 1860bp. The DNA ladder shown is the standard 1 Kbp ladder.

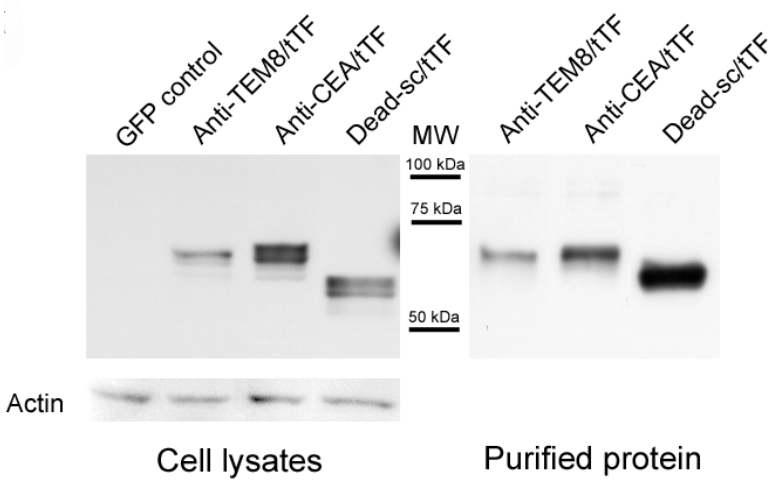

Figure 4-9. Fusion protein production and secretion. Western blot of protein expression in crude cell lysates and in purified culture medium from 293T cells transiently transfected with transposon vector DNA or GFP as a control. Thirty micrograms of cell lysate were loaded per lane and an anti-actin antibody was used as a loading control. A molecular weight (MW) ladder is shown between the blots.

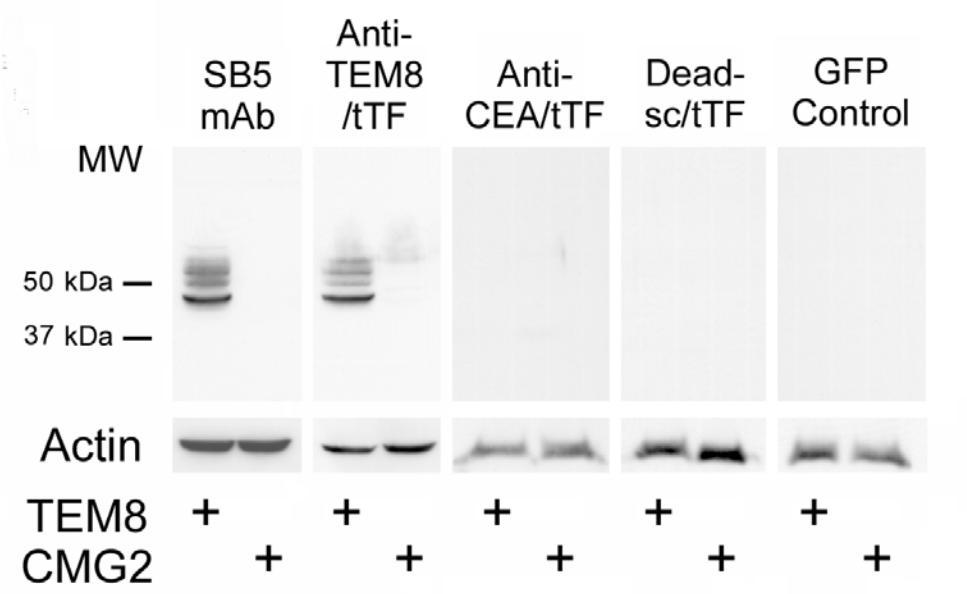

Figure 4-10. Anti-TEM8/tTF binding. Fusion protein recognition and binding to TEM8 was established by Western blot analysis. Separate Western blots containing cell lysates from 293T/TEM8 and 293T/CMG2 were probed with either the SB5 monoclonal antibody or medium from 293T cells transfected with Sleeping Beauty transposons expressing either the anti-TEM8/tTF, anti-CEA/tTF, Dead-sc/tTF or GFP proteins.

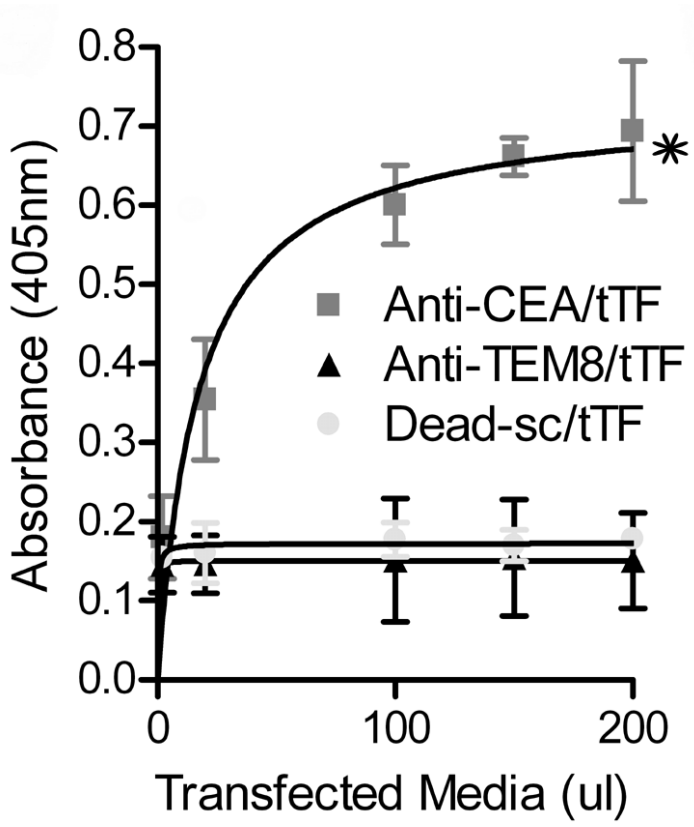

Figure 4-11. Anti-CEA/tTF indirect ELISA. Fusion protein recognition and binding of CEA was established by indirect ELISA. Different amounts of medium from 293T cells transfected with the Sleeping Beauty transposons expressing either anti-TEM8/tTF, anti-CEA/tTF, or Dead-sc/tTF were used to probe immobilized CEA on a 96 well microtiter plate. Results are shown as the mean optical density at 405nm of three separate experiments. $p = 0.0015$ as determined by an ANOVA.

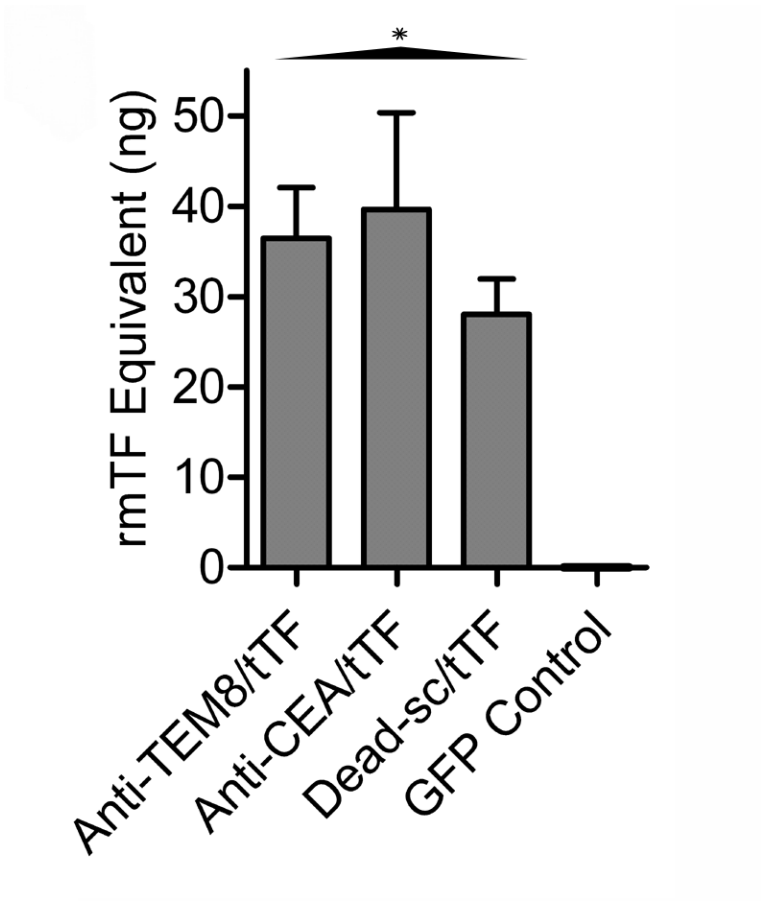

Figure 4-12. Tissue factor activity. Tissue factor activity was measured using a quantitative assay that measures the ability of tissue factor to cleave a colorimetric substrate. A standard curve was set up using serially diluted purified recombinant murine tissue factor (rmTF). Shown is the activity of the fusion proteins in rmTF equivalents as determined by the standard curve. The results presented here are the combination of three separate experiments. $p = 0.0011$ as determined by an ANOVA.

CHAPTER 5
IN VIVO EVALUATION OF THE FUSION PROTEIN PLASMIDS

Introduction

The SB constructs housing the fusion protein genes were evaluated in a xenograft model of human colorectal cancer using nude mice and the human colorectal carcinoma cell line HT-29. This model was chosen for its ease of reproducibility and because HT-29 cells are known to express CEA, and TEM8 was originally reported in colorectal carcinoma samples (24). Three types of experiments were designed to evaluate the fusion proteins, which included a tumor growth experiment, a tumor growth delay experiment and a circulating fusion protein experiment. The latter two experiments were based on the tumor growth experiment design (Figure 5-1) with minor changes that are described in Chapter 2. Analysis of these experiments determined whether or not the fusion proteins behaved *in vivo* in a manner the *in vitro* results predicted as well as gauging the anti-tumor effects of each the fusion protein.

Results

Characterization of the Xenograft Model of Human Colorectal Cancer

Prior to performing the gene delivery studies, we optimized tumor injections to the left hind limb so that untreated tumors would reach the size of ~1.3 cm^3 in 30 days. Immunohistochemistry was used to probe the expression patterns of both CEA and TEM8 in the tumors to ensure the presence of both antigens (Figure 5-2). Carcinoembryonic antigen expression occurred within tumor cells as contrasted with tumor vessels shown with CD31 staining (Figure 5-2A, arrowheads). Tumor Endothelial Marker 8 expression occurred in close association with tumor vasculature marked by the endothelial marker MECA32 leaving tumor cells unstained (Figure 5-2B). These results agree with the literature on the expression patterns for both proteins; however it is important to note that TEM8 expression did not always

colocalize with the pan-endothelial markers CD31 and MECA32. A finding further evaluated in later experiments.

Fusion Protein Expression in the Lung and Circulating Levels

Previous work in our laboratory has shown that non-viral gene delivery using systemic injections of DNA/polyethylenimine complexes predominately results in gene expression within the lung (73). A Western blot of lung tissue following gene delivery of our fusion proteins confirms expression within the lungs (Figure 5-3). A capture ELISA was used to demonstrate that once therapy is delivered, the fusion protein is detectable in the circulation at a peak concentration of 425 ng/ml three days after a second plasmid injection (Figure 5-4). Given such small amounts of the fusion protein within the circulation, we planned to use an experimental design that included multiple rounds of gene delivery to enhance protein expression.

Evaluation of the Fusion Proteins in the Xenograft Model of Human Colorectal Cancer

We first evaluated the fusion proteins in a tumor growth experiment (Figure 5-5). Tumor bearing animals were divided into four groups and given repeated weekly injections of the anti-TEM8/tTF, anti-CEA/tTF or the Dead-sc/tTF constructs. An untreated control group received no DNA injections. Tumor volume was assessed biweekly by taking three perpendicular measurements. By day 18, the anti-TEM8/tTF group showed a statistically significant response ($p < 0.05$) that only improved by day 30 ($p < 0.001$) when compared to the untreated control. The anti-CEA/tTF group reached a statistically significant result ($p < 0.01$) only at day 30 when compared to the untreated control. In addition, 15% of the anti-TEM8 group displayed a complete regression of tumor volume and was the only group to display such events. These results prompted us to perform a tumor growth delay study where animals received treatments once a week until their tumors surpassed 1.3 cm^3 (Figure 5-6). Anti-TEM8/tTF had a median tumor growth delay of 42.5 days ($p = 0.0367$), while the other groups fell within 28 +/- 2 days.

This result translates into a 49% increased delay time or 14 days when compared to the untreated control.

Tumor Localization of the Fusion Proteins

Treated tumors were assessed for evidence of fusion protein targeting, vessel density, and thrombosis. We first examined crude cell lysates from tumors of untreated animals and anti-TEM8/tTF treated animals for the presence of fusion proteins (Figure 5-7). After seeing a band corresponding to anti-TEM8/tTF, we examined all groups for tumor localization of the fusion proteins via immunohistochemistry. Both the anti-TEM8/tTF and anti-CEA/tTF fusion proteins localized in the tumor in a manner predicted by their antigen recognition (Figure 5-8). Anti-CEA/tTF staining was weaker than anti-TEM8 staining, but showed localization only to the tumor cells similar to the staining in Figure 5-2A. The anti-TEM8/tTF fusion protein localized to tumor vessels and/or stroma and excluded tumors cells in a manner similar to TEM8 staining in Figure 5-2B. Dead-sc/tTF and untreated controls showed no positive staining for fusion proteins, however, vessel staining and autofluorescent erythrocytes within vessels were present. These results suggest that the anti-TEM8/tTF and anti-CEA/tTF proteins homed to the tumor and bound their respective antigens.

Targeted Thrombosis

We examined H&E staining of tumor sections for evidence of thrombosis induced by the truncated tissue factor domain of our fusion proteins (Figure 5-9). Major thrombosis events only happened in the anti-TEM8/tTF and anti-CEA/tTF groups. For this experiment, we defined a thrombosis event as having both an aggregation of blood cells along with large areas of surrounding tumor necrosis. Aggregation of red blood cells alone or small areas of necrosis in the centers of the tumors were not considered a true thrombotic event.

Vessel Density

Previous reports indicate binding TEM8 or hindering its interaction with binding partners led to a decrease in vessel density implying TEM8 function is important for either vessel development or maintenance in tumors (44-46). We examined tumor vessel density in all groups utilizing MECA32 staining and found a 45% ($p = 0.005$) reduction in vessels for the anti-TEM8/tTF fusion protein treated animals when compared to Dead-sc/tTF, anti-CEA/tTF and untreated control (Figure 5-10).

TEM8 Colocalization

While characterizing protein expression within the xenograft model, we noticed TEM8 expression did not always colocalize with the known endothelial markers MECA32 and CD31; however, cells positive for TEM8 always associated with tumor vessels. This observation led us to hypothesize that there might be another population of cells associated with tumor vessels that were positive for TEM8, but were not endothelial cells. We examined tumor sections for colocalization of TEM8 with other known markers including pericytes (NG2), fibroblasts (SMA, FSP1), leukocytes (CD45) and hematopoietic stem cells (CD34). We observed that occasionally TEM8-positive cells colocalized with the endothelial marker MECA32 (Figure 5-11A, arrows), while a small population of TEM8-positive cells were also CD34 positive (Figure 5-11B, arrows). All of the other remaining markers were negative for colocalization.

Discussion

Since being discovered in 2000, TEM8 has emerged as an intriguing protein that differentiates tumor endothelial cells from normal endothelial cells. Selectively expressed proteins are invaluable in medicine and basic research since they can be used to specifically deliver therapeutic molecules to expressing cells. Recently, several reports suggested that targeting TEM8 *in vivo* may have a benefit in cancer therapy, but these articles either

nonspecifically targeted TEM8 using parts of the anthrax toxin or prevented TEM8 from binding a physiological partner (44-46). In addition, these reports did not analyze the expression pattern of TEM8 in their animal model leaving to question whether TEM8 expression patterns are equivalent in mice and humans. In this chapter, we provided evidence of the treatment of solid tumors by utilizing the Sleeping Beauty transposon system to deliver a gene encoding a fusion protein that once expressed was able to target TEM8 and disrupt the tumor vasculature *in vivo*.

First, we confirmed that our anti-TEM8/tTF fusion protein exclusively bound TEM8 *in vitro*. To date, the only other therapy capable of specific TEM8 targeting is a mutated version of protective antigen that has not been tested *in vivo* (181). Demonstrating specificity for TEM8 is important since TEM8 and CMG2 share a 60% homology within their extracellular domains and both are functional anthrax toxin receptors (30, 31). Therapies should be evaluated for specific targeting of TEM8 to circumvent unintended systemic damage since CMG2 is reported as being widely expressed in tissues (31).

Our *in vivo* experiments with the anti-TEM8/tTF transposon construct achieved a tumor growth inhibition of ~55% and slowed the progression of tumors by at least 49%. These results are consistent with similar studies that treated tumors with fusion proteins that delivered truncated tissue factor as a vascular disrupting agent (174, 180, 182). However, our study differs from previous reports since we used a transposon gene delivery approach as opposed to purified protein. The peak circulating concentration of our fusion protein after two gene deliveries was 425 ng/ml. This concentration is far less than that achieved by viral vectors expressing similar fusion proteins *in vivo* (183) and almost twenty-five times less than that used when similar fusion proteins are delivered by direct injection (174, 180, 182). Despite this low circulating concentration, we still generated a significant result with respect to tumor growth and illustrated

the anti-tumor effects of anti-TEM8/tTF by providing evidence of homing, tumor vessel localization, a decrease in tumor vessel density and targeted thrombosis. We anticipate that delivery of purified anti-TEM8 fusion proteins will potentiate the anti-tumor effect and may lead to a more robust tumor regression.

A decrease in tumor vessel density is a common theme in studies trying to target TEM8. The mere binding of TEM8 or preventing TEM8 from binding a physiological partner seems enough to decrease tumor vessel density. For strategies utilizing anthrax toxin components, the outcome may be explained by protective antigen forming a pore in cell membranes that disrupts metabolic activity and causes cell swelling (184). In the case of therapeutic molecules that either bind TEM8 or block interaction with a physiological partner, their effect may be explained by a possible role for TEM8 in the VEGF pathway (43). Thus, the strategy in this report may have unintentionally had a two pronged antitumor response, which may have led to the achievement of a statistically significant result despite the low circulating protein levels.

Finally, the literature supports the assumption that TEM8 is strictly a marker of tumor endothelium. However, early in our studies we noticed that TEM8 expression did not always colocalize with the pan-endothelial markers MECA32 or CD31. In some instances TEM8 expression occurred adjacent to endothelial cells in the tumor vessels. This led us to hypothesize that other cell types may be TEM8 positive and we examined TEM8 colocalization with non-endothelial cell mesenchymal markers. Our results confirmed that some TEM8 positive cells are of endothelial origin, but also revealed that a small percentage of TEM8 positive cells colocalize with CD34. This outcome supports the recent findings of another group reporting TEM8 expression in stimulated endothelial progenitor cells (185). This result also supports the idea of endothelial progenitor cells giving aid to distressed tumors by helping the formation of new

vasculature (186, 187). This is a controversial topic within the literature since the magnitude of support provided by EPCs during tumor angiogenesis may be different in mice and humans (188). Regardless of the exact location of TEM8, our studies demonstrate that targeting this protein does influence tumor growth and progression.

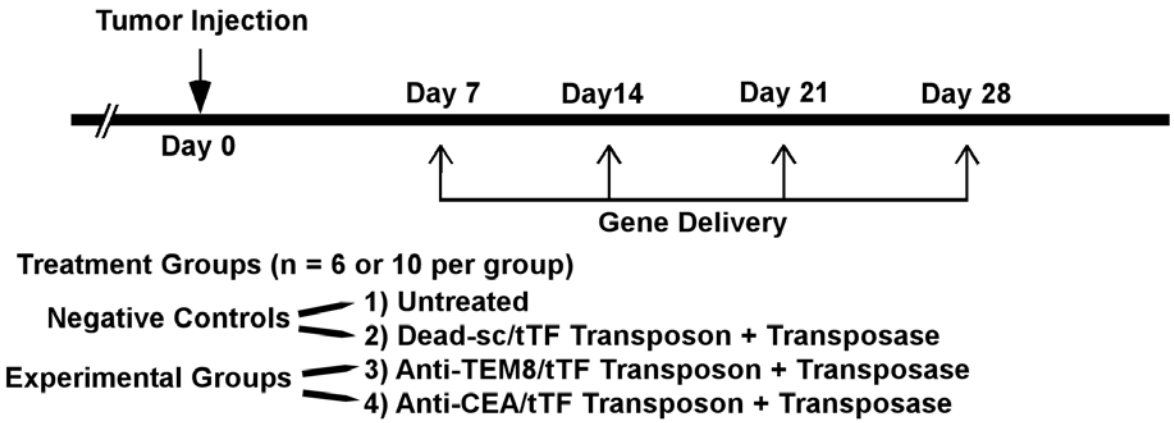

Figure 5-1. Tumor growth experiment. Schematic diagram illustrates the timing of tumor implantation and subsequent gene delivery. Animals were sacrificed at Day 30 or when tumors grew to maximum size of 1.3 cm^3.

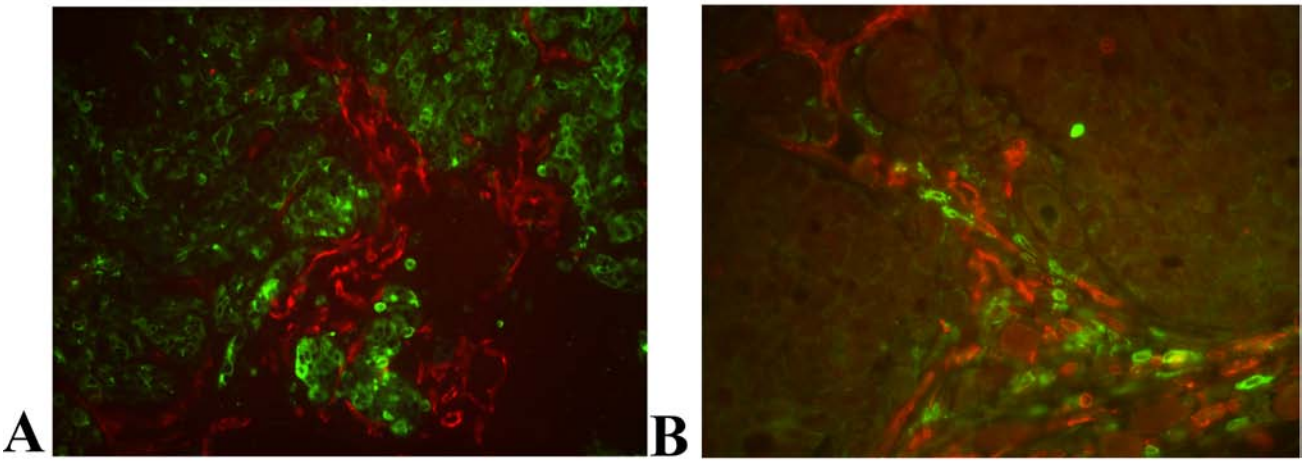

Figure 5-2. Tumor characterization. A) CEA expression (green) contrasted by vessel staining with CD31 (red) shows CEA expression is limited to tumor cells. B) TEM8 expression (green) contrasted by vessel staining with MECA32 (red) shows TEM8 expression localizes close to tumor vasculature.

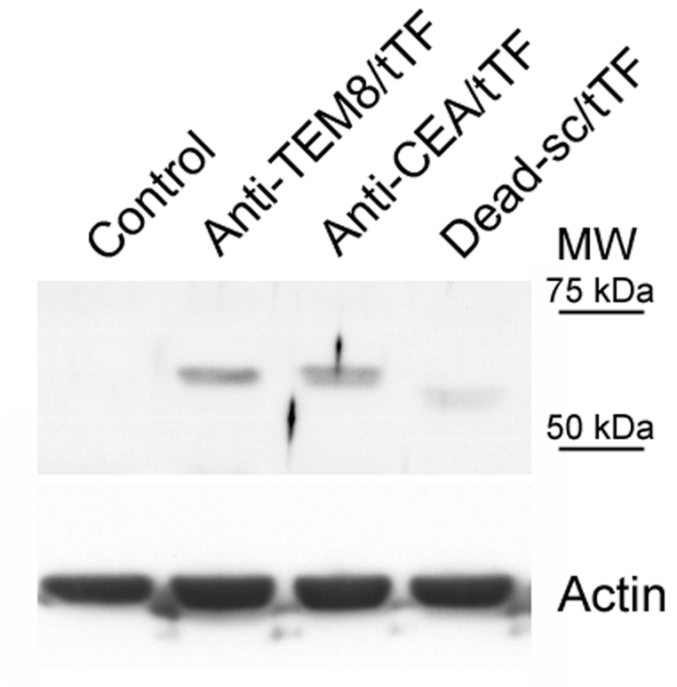

Figure 5-3. Fusion protein expression in the lung. Western blots were performed on lung tissue from gene treated animals. Fusion protein expression was detected at low levels in the correct size range. Actin expression is shown to indicate equal protein loading.

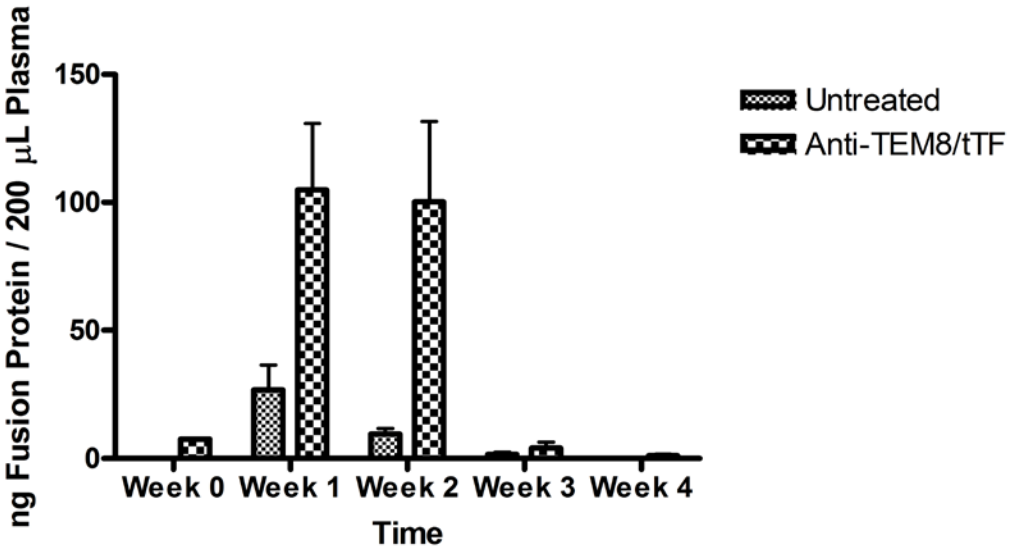

Figure 5-4. Circulating anti-TEM8/tTF. Using a sandwich ELISA, the concentration of the anti-TEM8/tTF fusion protein within plasma was determined following gene delivery. Shown is an average value from two independent experiments performed in duplicate.

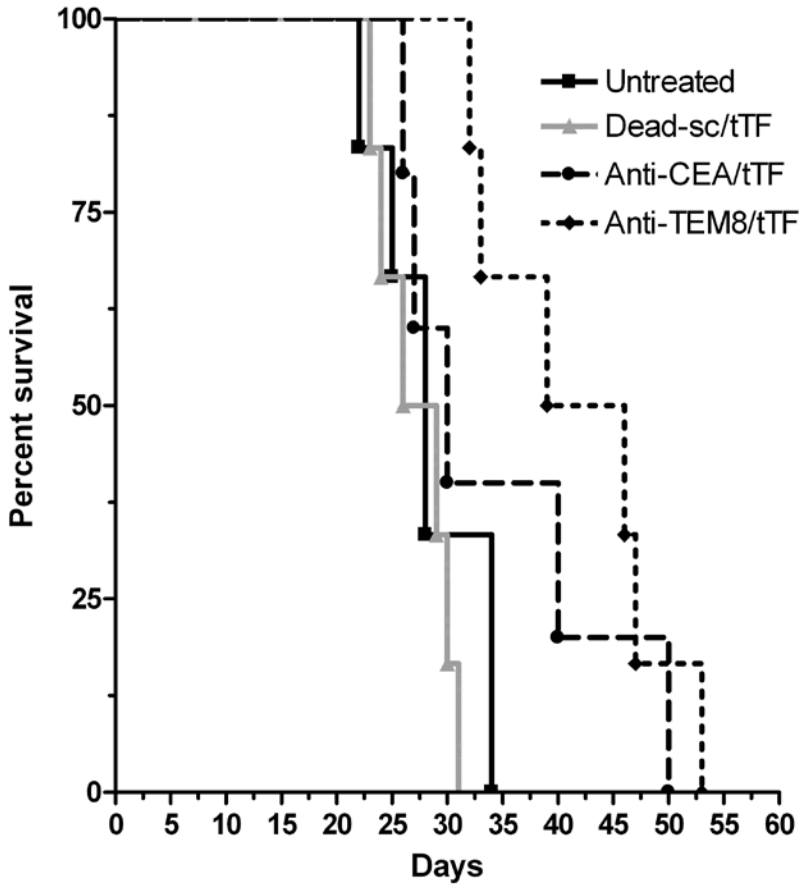

Figure 5-6. Tumor growth delay curve. Animals received weekly gene delivery until the tumor reached 1.3 cm^3 (n=6 per group; anti-CEA/tTF had one censored animal). Anti-TEM8/tTF treated animals had a median tumor growth delay of 42.5 days (p = 0.0367) compared to 28 days for untreated.

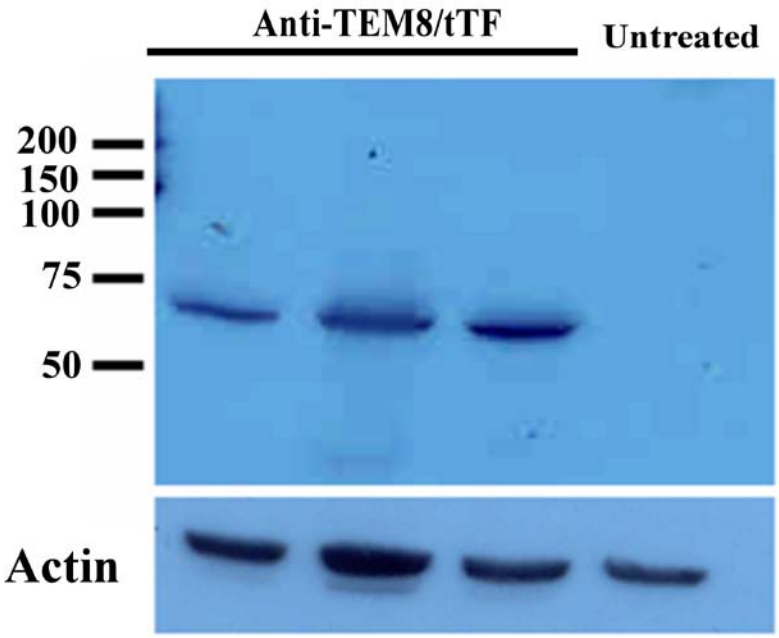

Figure 5-7. Fusion protein homing to tumor. Western blot analysis of crude cell lysates from tumor tissue detected the anti-TEM8/tTF fusion protein in samples taken from mice treated with the anti-TEM8/tTF transposon plasmid. Samples from untreated control animals did not yield a band.

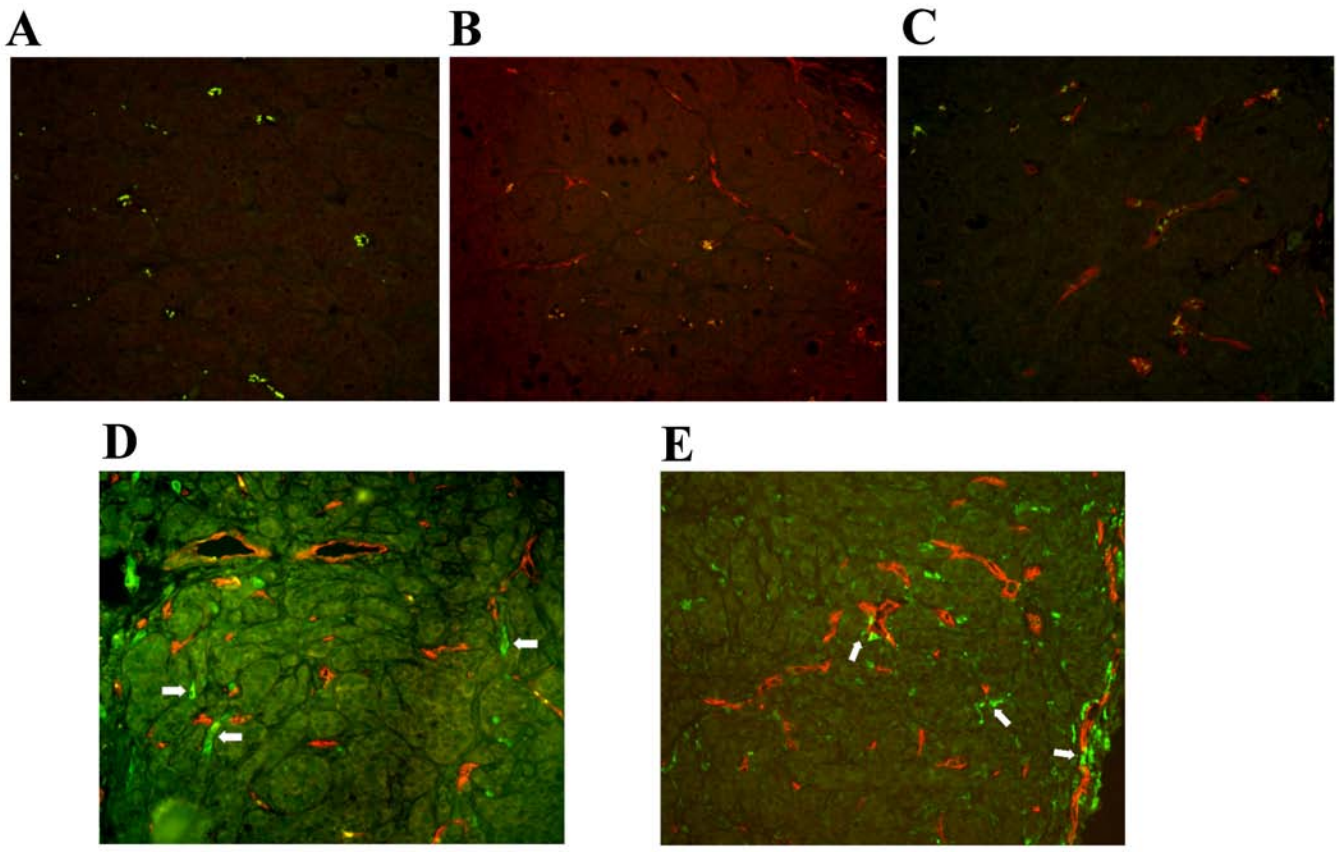

Figure 5-8. Fusion protein localization in tumor tissue. A) Nonspecific IgG control. Autoflourescent erythrocytes can be seen in the lumen of vessels. Neither vessels (red) nor fusion protein (green) staining is present. B) Untreated control animal sections stained positive for vessels only. C) Sections from animals treated with the transposon plasmid carrying the gene for Dead-sc/tTF stained red for vessels, but no fusion protein is present within the tumor. D) Sections from animals treated with the transposon plasmid carrying the gene for anti-CEA/tTF stained red for vessels and some tumor cells stained green for the fusion protein (arrows). E) Sections from animals treated with the transposon plasmid carrying the gene for anti-TEM8/tTF stained red for vessels and some cells nearby vessels stained green for the fusion protein (arrows).

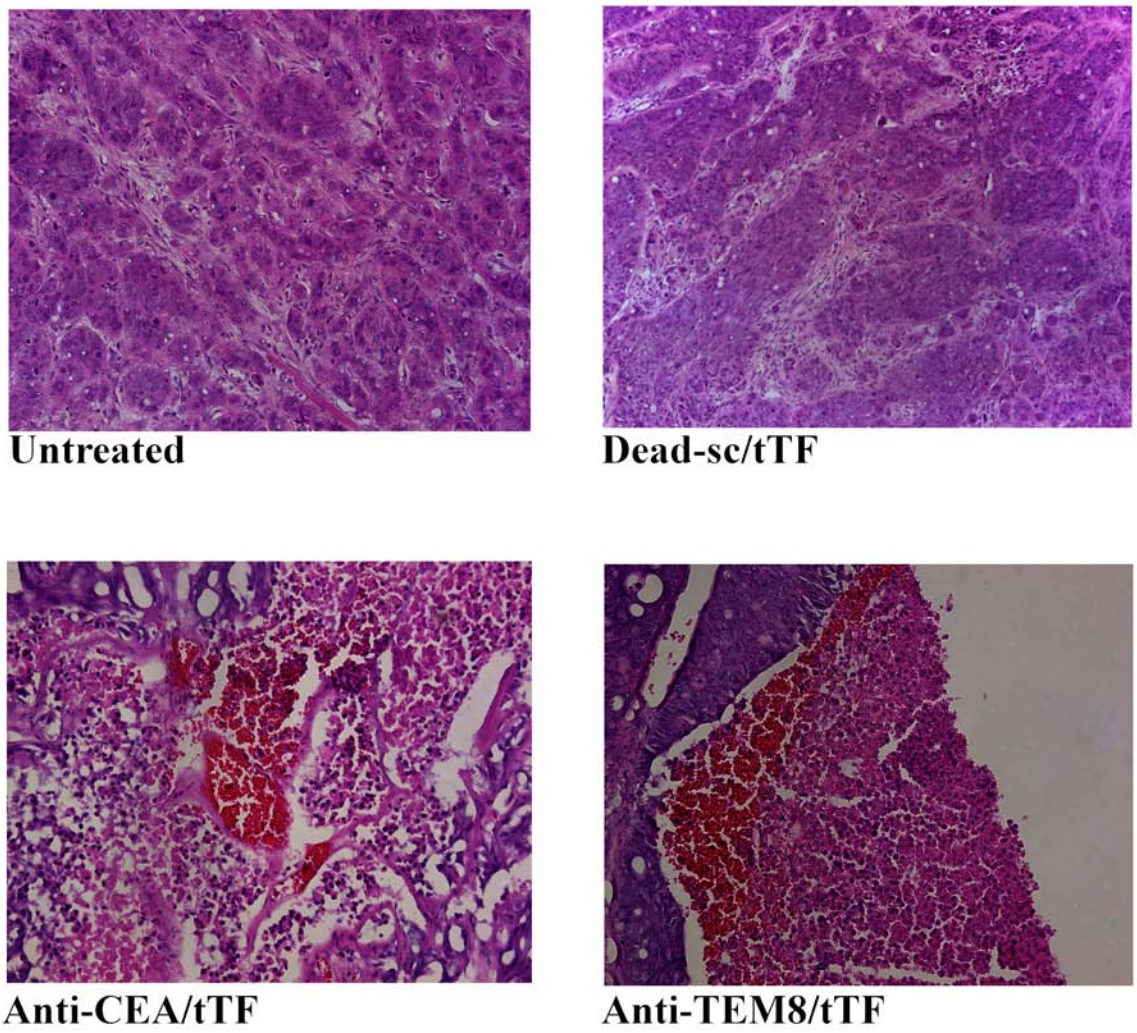

Figure 5-9. Targeted thrombosis. Histological analysis of xenograft tumors to assess for targeted thrombosis events after 30 days of treatment. Tumors from mice treated with the transposons carrying the gene for anti-TEM8/tTF and anti-CEA/tTF displayed visible instances of thrombosis in their outer edge without the aid of histology during sample preparation. H & E staining of these samples examined at 20x magnification showed areas of red blood cell accumulation and were accompanied by large areas of necrosis and tissue fragmentation. Tumors from untreated control animals and animals treated with a transposon carrying the gene for Dead-sc/tTF did not show evidence of targeted thrombosis.

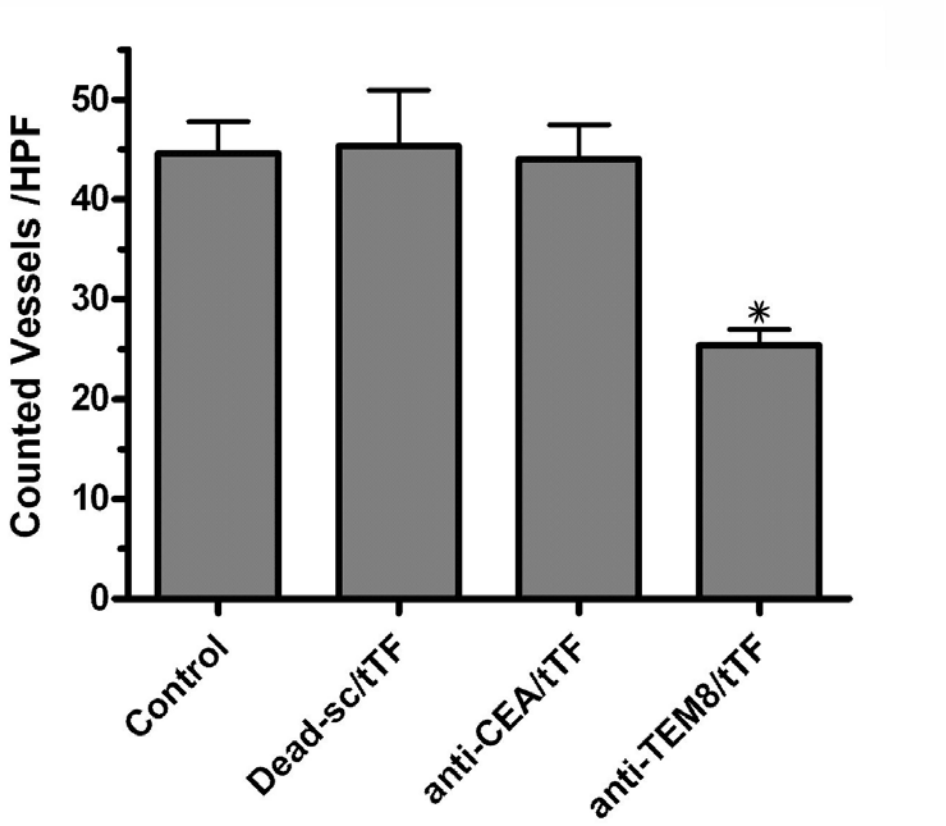

Figure 5-10. Vessel density. Vessel density was determined by staining tumor sections with MECA 32 and counting individual vessels at 20x magnification. Tumors in mice treated with anti-TEM8/tTF exhibited a 45% reduction in vessels density when compared to untreated, Dead-sc/tTF or anti-CEA/tTF. *p = 0.005 as determined by ANOVA.

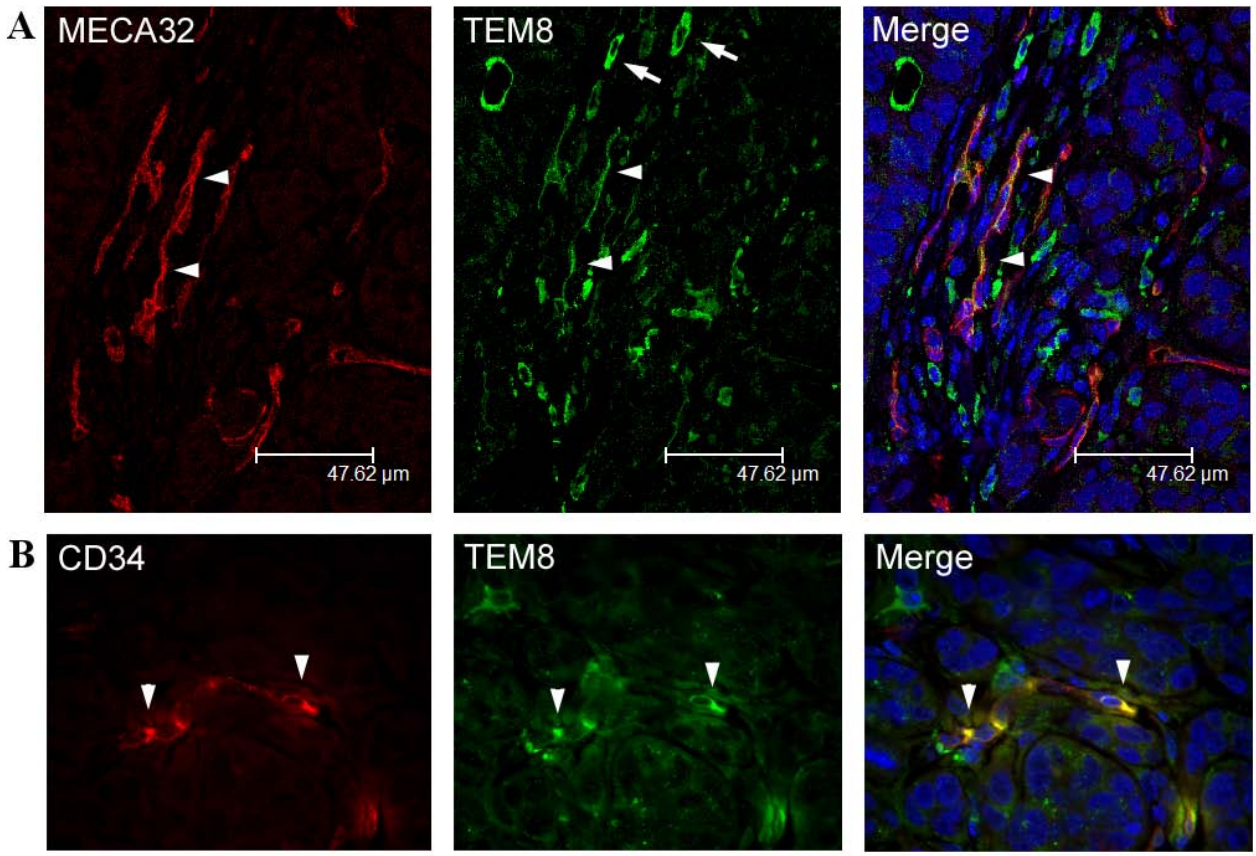

Figure 5-11. TEM8 colocalization. Colocalization of TEM8 with markers of endothelial cells and hematopoietic stem cells. Immunohistochemistry analysis with confocal microscopy was used to better characterize the localization of the TEM8 antigen in the tumor microenvironment. A) Colocalization of TEM8 (green) and MECA 32 (red) could be observed (arrowheads), however there were clearly cells that did not colocalize (arrows). B) Colocalization of TEM8 (green) with the hematopoietic stem cell marker CD34 (red) was also observed, however not all CD34 positive cells were TEM8 positive.

CHAPTER 6
SUMMARY, ANALYSIS AND FUTURE DIRECTIONS

Summary

The initiation of this doctoral work began with a review of the literature that produced reports describing a new area of cancer research that examines mesenchymal cell populations participating in tumor establishment and growth. Some of these reports tried to elucidate novel markers on these cells creating a new niche for therapies against cancer. In Chapter 1, a background in cancer trends and therapy was discussed as an introduction to a new area of cancer research called the tumor microenvironment. The chapter proceeded with a description of the tumor microenvironment and how the tumor influences its development. This description progressed to the idea that stromal cells influenced by the tumor have aberrant patterns of protein expression like that of tumor cells and their upregulation of tumor markers. The chapter ended with the introduction of TEM8 and an overview of this study. Chapter 2 discussed in detail the methods used to complete this doctoral work. Chapter 3 was a review of the literature on the Sleeping Beauty Transposon System. This chapter discussed the interaction between the transposon and transposase to facilitate DNA integration in nature as well as how it is now exploited for gene therapy and gene discovery. The end of Chapter 3 summarized many of the gene therapy experiments conducted with SB and highlighted the first ever clinical trial with this vector. Chapter 4 began with a synopsis of fusion proteins and their domains, which led to the design of the fusion proteins used in this research. This chapter catalogued the creation of the anti-TEM8/tTF, anti-CEA/tTF and Dead-sc/tTF fusion proteins and gave evidence of the activity for each of their domains *in vitro*. Chapter 5 discussed the *in vivo* results of this doctoral work. First, the xenograft model of colorectal cancer was characterized for its reproducibility and expression of the target antigens CEA and TEM8. Next, this chapter examined the therapeutic

results of each fusion protein in the animal model and characterized the effects of the fusion proteins to the tumor both macroscopically and microscopically. Together, these chapters presented a logical sequence of steps that identified TEM8 as a means to target tumor vasculature and developed an effective therapy utilizing that means.

Analysis

The achievements produced by this doctoral work are four fold. First, a strategy was developed that discerns TEM8 from CMG2 by creating a fusion protein using a scFv against TEM8 as the targeting domain. No other reports have shown this distinction and then evaluated their therapy both *in vitro* and *in vivo*. The advantages offered by using scFvs are multiple due to both the affinity for a specific ligand and their simplicity for incorporation into fusion proteins. In addition, scFvs are well established in the clinic as therapeutic molecules generally well tolerated in the treatment or visualization of disease (171). Most other strategies targeting TEM8 utilize protective antigen, which could bind either anthrax toxin receptor (30, 31). This possibility has serious implications for use in the clinic due to both the macabre actions of anthrax toxin and recognition of the toxin components by the immune system.

Second, this report was the first to evaluate the specific targeting of TEM8 in tumor vessels to deliver potent therapeutic molecules. Until now, the therapeutic value of specifically targeting TEM8 in tumor vessels has been pure conjecture since CMG2 is also expressed and therapies could not distinguish between the two. The results presented in this work clearly show that guiding therapeutic molecules to tumor vessels by targeting TEM8 yields encouraging results for cancer treatment. In addition, this work supports similar findings in the literature that binding TEM8 or keeping it from interacting with a physiological partner is therapeutic by decreasing vessel density in the tumor.

Third, this research showed that SB is capable of producing sufficient amounts of therapeutic protein to treat an established solid tumor when delivered in an academic setting. This report is the first time a tumor was treated successfully with systemic administration of SB . Despite the positive result though, there is plenty of room for improvement when considering circulating levels were 25 times less than that achieved by purified protein injection.

Finally, this work examined the expression of TEM8 in the tumor tissue. The results established TEM8 localizes to tumor vessels, but other mesenchymal cell populations were positive for TEM8 besides endothelial cells. This is the first report to show another population of TEM8 positive cells within malignant lesions. Our results did not conclusively identify a single specific cell population, but we did show evidence of TEM8 co localizing with CD34 indicating a possible cell type of hematopoietic lineage.

Future Directions

This doctoral work established that specific targeting of TEM8 is a novel anti-cancer strategy that can be used to deliver powerful vascular disrupting agents to tumor vessels. The main limitation of this work was the dependence upon gene delivery and integration to produce the fusion proteins. Sleeping Beauty gene delivery is hindered by low expression levels. Even though the circulating levels of anti-TEM8/tTF were sufficient to yield a significant therapeutic response, that response required a weekly gene delivery injection. Viral mediated gene delivery is capable of 2 to 20 times the peak circulating levels achieved by SB with just one injection. Future work should focus on injecting purified fusion protein. This strategy allows for consistent delivery of therapeutic molecules at high circulating concentrations. The results of this doctoral work might have benefited from purified protein injection since the goal was to infarct the tumor vasculature with tTF; a tissue factor derivative that is 5 orders of magnitude less active. The possibility exists that peak circulating levels of the anti-TEM8/tTF fusion protein were

insufficient to bind all TEM8 present within the tumor vasculature reducing the therapeutic response. Lastly, if targeting TEM8 enters clinical trials, injecting purified protein would alleviate many safety concerns associated with gene delivery integration and recognition by the immune system.

Another area for future consideration is evolving the therapeutic approach for targeting TEM8. Both the results in this study and in the literature support the idea that binding the extracellular domain of TEM8 is therapeutic. This consistent outcome makes TEM8 an ideal target for a small molecule antagonist. Furthermore, the cytoplasmic tail of TEM8 has multiple possible phosphorylation sites that could also be therapeutic targets given the recent implication that TEM8 plays a role in the VEGF pathway (45). Changing the effector domain on the anti-TEM8 scFv is another strategy for consideration. The results presented here showed TEM8 expression localized to tumor vessels in our xenograft model and that TEM8 expression was not limited to just endothelial cells. This finding supports exploration into developing additional effector molecules that could have detrimental effects on the tumor by influencing the surrounding microenvironment such as interleukin-2, interleukin-24 or simply radio-labeling the anti-TEM8 scFv.

Finally, the last future direction encouraged by this work is the elucidation of the physiological function of TEM8 in either tumor vasculature or embryogenesis. Most of what has been determined about TEM8 came from groups studying anthrax toxin entry into cells. Very few groups have looked at involvement of TEM8 in known pathways. The studies that have looked into TEM8 function produced conflicting results that do not have widespread acceptance. Determining the physiological role of TEM8 has many possible benefits including the discovery

of a possible pathway crucial for tumor angiogenesis and a binding partner that would be an immediate target for cancer therapy.

LIST OF REFERENCES

1. AmericanCancerSociety Cancer Facts and Figures 2008. Cancer Facts and Figures 2008. 2008.

2. Nelson, H., Petrelli, N., Carlin, A., et al. Guidelines 2000 for colon and rectal cancer surgery. J Natl Cancer Inst 2001;93:583-96.

3. Gerber, D. E. and Chan, T. A. Recent advances in radiation therapy. Am Fam Physician 2008;78:1254-62.

4. Field, K. M., Dow, C., and Michael, M. Part I: Liver function in oncology: biochemistry and beyond. Lancet Oncol 2008;9:1092-101.

5. Field, K. M. and Michael, M. Part II: Liver function in oncology: towards safer chemotherapy use. Lancet Oncol 2008;9:1181-90.

6. Colozza, M., de Azambuja, E., Personeni, N., et al. Achievements in systemic therapies in the pregenomic era in metastatic breast cancer. Oncologist 2007;12:253-70.

7. Argento, M., Hoffman, P., and Gauchez, A. S. Ovarian cancer detection and treatment: current situation and future prospects. Anticancer Res 2008;28:3135-8.

8. Moon, C., Park, J. C., Chae, Y. K., Yun, J. H., and Kim, S. Current status of experimental therapeutics for prostate cancer. Cancer Lett 2008;266:116-34.

9. Caspi, R. R. Immunotherapy of autoimmunity and cancer: the penalty for success. Nat Rev Immunol 2008;8:970-6.

10. Nahta, R. and Esteva, F. J. Trastuzumab: triumphs and tribulations. Oncogene 2007;26:3637-43.

11. Pantaleo, M. A., Nannini, M., Lopci, E., et al. Molecular imaging and targeted therapies in oncology: new concepts in treatment response assessment. a collection of cases. Int J Oncol 2008;33:443-52.

12. Savage, D. G. and Antman, K. H. Imatinib mesylate--a new oral targeted therapy. N Engl J Med 2002;346:683-93.

13. Adams, G. P. and Weiner, L. M. Monoclonal antibody therapy of cancer. Nat Biotechnol 2005;23:1147-57.

14. Kerbel, R. S. Tumor angiogenesis. N Engl J Med 2008;358:2039-49.

15. Vogelstein, B. and Kinzler, K. W. Cancer genes and the pathways they control. Nat Med 2004;10:789-99.

16. Whiteside, T. L. The tumor microenvironment and its role in promoting tumor growth. Oncogene 2008;27:5904-12.

17. Orimo, A. and Weinberg, R. A. Stromal fibroblasts in cancer: a novel tumor-promoting cell type. Cell Cycle 2006;5:1597-601.

18. Olumi, A. F., Grossfeld, G. D., Hayward, S. W., et al. Carcinoma-associated fibroblasts direct tumor progression of initiated human prostatic epithelium. Cancer Res 1999;59:5002-11.

19. Folkman, J. Tumor angiogenesis: therapeutic implications. N Engl J Med. 1971;285:1182-6.

20. Folkman, J. What is the evidence that tumors are angiogenesis dependent? J Natl Cancer Inst. 1990;82:4-6.

21. Ribatti, D., Vacca, A., and Dammacco, F. New non-angiogenesis dependent pathways for tumour growth. Eur J Cancer 2003;39:1835-41.

22. Bergers, G. and Benjamin, L. E. Tumorigenesis and the angiogenic switch. Nat Rev Cancer 2003;3:401-10.

23. Donnem, T., Al-Saad, S., Al-Shibli, K., et al. Inverse prognostic impact of angiogenic marker expression in tumor cells versus stromal cells in non small cell lung cancer. Clin Cancer Res 2007;13:6649-57.

24. St Croix, B., Rago, C., Velculescu, V., et al. Genes expressed in human tumor endothelium. Science. 2000;289:1197-202.

25. van Beijnum, J. R., Dings, R. P., van der Linden, E., et al. Gene expression of tumor angiogenesis dissected: specific targeting of colon cancer angiogenic vasculature. Blood. 2006;108:2339-48. Epub 006 Jun 22.

26. Samara, R. N., Laguinge, L. M., and Jessup, J. M. Carcinoembryonic antigen inhibits anoikis in colorectal carcinoma cells by interfering with TRAIL-R2 (DR5) signaling. Cancer Res 2007;67:4774-82.

27. Hammarstrom, S. The carcinoembryonic antigen (CEA) family: structures, suggested functions and expression in normal and malignant tissues. Semin Cancer Biol. 1999;9:67-81.

28. Ruibal Morell, A. CEA serum levels in non-neoplastic disease. Int J Biol Markers 1992;7:160-6.

29. Carson-Walter, E. B., Watkins, D. N., Nanda, A., et al. Cell surface tumor endothelial markers are conserved in mice and humans. Cancer Res. 2001;61:6649-55.

30. Bradley, K. A., Mogridge, J., Mourez, M., Collier, R. J., and Young, J. A. Identification of the cellular receptor for anthrax toxin. Nature 2001;414:225-9.

31. Scobie, H. M., Rainey, G. J., Bradley, K. A., and Young, J. A. Human capillary morphogenesis protein 2 functions as an anthrax toxin receptor. Proc Natl Acad Sci U S A. 2003;100:5170-4. Epub 2003 Apr 16.

32. Hotchkiss, K. A., Basile, C. M., Spring, S. C., et al. TEM8 expression stimulates endothelial cell adhesion and migration by regulating cell-matrix interactions on collagen. Exp Cell Res 2005;305:133-44.

33. Rmali, K. A., Puntis, M. C., and Jiang, W. G. TEM-8 and tubule formation in endothelial cells, its potential role of its vW/TM domains. Biochem Biophys Res Commun. 2005;334:231-8.

34. Werner, E., Kowalczyk, A. P., and Faundez, V. Anthrax toxin receptor 1/tumor endothelium marker 8 mediates cell spreading by coupling extracellular ligands to the actin cytoskeleton. J Biol Chem 2006;281:23227-36.

35. Nanda, A., Carson-Walter, E. B., Seaman, S., et al. TEM8 interacts with the cleaved C5 domain of collagen alpha 3(VI). Cancer Res 2004;64:817-20.

36. Go, M. Y., Chow, E. M., and Mogridge, J. The Cytoplasmic Domain of Anthrax Toxin Receptor 1 Affects Binding of Protective Antigen. Infect Immun 2008.

37. Dickeson, S. K. and Santoro, S. A. Ligand recognition by the I domain-containing integrins. Cell Mol Life Sci. 1998;54:556-66.

38. Sakai, Y., Goodison, S., Kusmartsev, S., et al. Bcl-2 mediated modulation of vascularization in prostate cancer xenografts. Prostate 2009;69:459-70.

39. Davies, G., Cunnick, G. H., Mansel, R. E., Mason, M. D., and Jiang, W. G. Levels of expression of endothelial markers specific to tumour-associated endothelial cells and their correlation with prognosis in patients with breast cancer. Clin Exp Metastasis 2004;21:31-7.

40. Davies, G., Rmali, K. A., Watkins, G., et al. Elevated levels of tumour endothelial marker-8 in human breast cancer and its clinical significance. Int J Oncol 2006;29:1311-7.

41. Rmali, K. A., Puntis, M. C., and Jiang, W. G. Prognostic values of tumor endothelial markers in patients with colorectal cancer. World J Gastroenterol 2005;11:1283-6.

42. Rmali, K. A., Watkins, G., Harrison, G., et al. Tumour endothelial marker 8 (TEM-8) in human colon cancer and its association with tumour progression. Eur J Surg Oncol 2004;30:948-53.

43. Jinnin, M., Medici, D., Park, L., et al. Suppressed NFAT-dependent VEGFR1 expression and constitutive VEGFR2 signaling in infantile hemangioma. Nat Med 2008;14:1236-46.

44. Duan, H. F., Hu, X. W., Chen, J. L., et al. Antitumor activities of TEM8-Fc: an engineered antibody-like molecule targeting tumor endothelial marker 8. J Natl Cancer Inst 2007;99:1551-5.

45. Rogers, M. S., Christensen, K. A., Birsner, A. E., et al. Mutant anthrax toxin B moiety (protective antigen) inhibits angiogenesis and tumor growth. Cancer Res 2007;67:9980-5.

46. Rouleau, C., Menon, K., Boutin, P., et al. The systemic administration of lethal toxin achieves a growth delay of human melanoma and neuroblastoma xenografts: assessment of receptor contribution. Int J Oncol 2008;32:739-48.

47. Bird, R. E., Hardman, K. D., Jacobson, J. W., et al. Single-chain antigen-binding proteins. Science. 1988;242:423-6.

48. Stone, M. J., Ruf, W., Miles, D. J., Edgington, T. S., and Wright, P. E. Recombinant soluble human tissue factor secreted by Saccharomyces cerevisiae and refolded from Escherichia coli inclusion bodies: glycosylation of mutants, activity and physical characterization. Biochem J. 1995;310:605-14.

49. Whitlow, M., Bell, B. A., Feng, S. L., et al. An improved linker for single-chain Fv with reduced aggregation and enhanced proteolytic stability. Protein Eng. 1993;6:989-95.

50. Huston, J. S., Levinson, D., Mudgett-Hunter, M., et al. Protein engineering of antibody binding sites: recovery of specific activity in an anti-digoxin single-chain Fv analogue produced in Escherichia coli. Proc Natl Acad Sci U S A 1988;85:5879-83.

51. Horton, R. M., Hunt, H. D., Ho, S. N., Pullen, J. K., and Pease, L. R. Engineering hybrid genes without the use of restriction enzymes: gene splicing by overlap extension. Gene 1989;77:61-8.

52. Fletcher, B. S., Dragstedt, C., Notterpek, L., and Nolan, G. P. Functional cloning of SPIN-2, a nuclear anti-apoptotic protein with roles in cell cycle progression. Leukemia 2002;16:1507-18.

53. Plasterk, R. H., Izsvak, Z., and Ivics, Z. Resident aliens: the Tc1/mariner superfamily of transposable elements. Trends Genet. 1999;15:326-32.

54. Ivics, Z., Izsvak, Z., Minter, A., and Hackett, P. B. Identification of functional domains and evolution of Tc1-like transposable elements. Proc Natl Acad Sci U S A 1996;93:5008-13.

55. Ivics, Z., Hackett, P. B., Plasterk, R. H., and Izsvak, Z. Molecular reconstruction of Sleeping Beauty, a Tc1-like transposon from fish, and its transposition in human cells. Cell 1997;91:501-10.

56. Converse, A. D., Belur, L. R., Gori, J. L., et al. Counterselection and co-delivery of transposon and transposase functions for Sleeping Beauty-mediated transposition in cultured mammalian cells. Biosci Rep 2004;24:577-94.

57. Geurts, A. M., Yang, Y., Clark, K. J., et al. Gene transfer into genomes of human cells by the sleeping beauty transposon system. Mol Ther 2003;8:108-17.

58. Heggestad, A. D., Notterpek, L., and Fletcher, B. S. Transposon-based RNAi delivery system for generating knockdown cell lines. Biochem Biophys Res Commun 2004;316:643-50.

59. Izsvak, Z., Ivics, Z., and Plasterk, R. H. Sleeping Beauty, a wide host-range transposon vector for genetic transformation in vertebrates. J Mol Biol 2000;302:93-102.

60. Clark, K. J., Geurts, A. M., Bell, J. B., and Hackett, P. B. Transposon vectors for gene-trap insertional mutagenesis in vertebrates. Genesis 2004;39:225-33.

61. Davidson, A. E., Balciunas, D., Mohn, D., et al. Efficient gene delivery and gene expression in zebrafish using the Sleeping Beauty transposon. Dev Biol 2003;263:191-202.

62. Wadman, S. A., Clark, K. J., and Hackett, P. B. Fishing for answers with transposons. Mar Biotechnol (NY) 2005;7:135-41.

63. Dupuy, A. J., Clark, K., Carlson, C. M., et al. Mammalian germ-line transgenesis by transposition. Proc Natl Acad Sci U S A 2002;99:4495-9.

64. Carlson, C. M., Dupuy, A. J., Fritz, S., et al. Transposon mutagenesis of the mouse germline. Genetics 2003;165:243-56.

65. Dupuy, A. J., Fritz, S., and Largaespada, D. A. Transposition and gene disruption in the male germline of the mouse. Genesis 2001;30:82-8.

66. Fischer, S. E., Wienholds, E., and Plasterk, R. H. Regulated transposition of a fish transposon in the mouse germ line. Proc Natl Acad Sci U S A 2001;98:6759-64.

67. Horie, K., Kuroiwa, A., Ikawa, M., et al. Efficient chromosomal transposition of a Tc1/mariner- like transposon Sleeping Beauty in mice. Proc Natl Acad Sci U S A 2001;98:9191-6.

68. Horie, K., Yusa, K., Yae, K., et al. Characterization of Sleeping Beauty transposition and its application to genetic screening in mice. Mol Cell Biol 2003;23:9189-207.

69. Luo, G., Ivics, Z., Izsvak, Z., and Bradley, A. Chromosomal transposition of a Tc1/mariner-like element in mouse embryonic stem cells. Proc Natl Acad Sci U S A 1998;95:10769-73.

70. Tolar, J., Osborn, M., Bell, S., et al. Real-time in vivo imaging of stem cells following transgenesis by transposition. Mol Ther 2005;12:42-8.

71. Belur, L. R., Frandsen, J. L., Dupuy, A. J., et al. Gene insertion and long-term expression in lung mediated by the Sleeping Beauty transposon system. Mol Ther 2003;8:501-7.

72. He, C. X., Shi, D., Wu, W. J., et al. Insulin expression in livers of diabetic mice mediated by hydrodynamics-based administration. World J Gastroenterol 2004;10:567-72.

73. Liu, L., Sanz, S., Heggestad, A. D., et al. Endothelial targeting of the Sleeping Beauty transposon within lung. Mol Ther. 2004;10:97-105.

74. Montini, E., Held, P. K., Noll, M., et al. In vivo correction of murine tyrosinemia type I by DNA-mediated transposition. Mol Ther 2002;6:759-69.

75. Ohlfest, J. R., Demorest, Z. L., Motooka, Y., et al. Combinatorial antiangiogenic gene therapy by nonviral gene transfer using the sleeping beauty transposon causes tumor regression and improves survival in mice bearing intracranial human glioblastoma. Mol Ther 2005;12:778-88.

76. Ohlfest, J. R., Frandsen, J. L., Fritz, S., et al. Phenotypic correction and long-term expression of factor VIII in hemophilic mice by immunotolerization and nonviral gene transfer using the Sleeping Beauty transposon system. Blood 2005;105:2691-8.

77. Ortiz-Urda, S., Lin, Q., Yant, S. R., et al. Sustainable correction of junctional epidermolysis bullosa via transposon-mediated nonviral gene transfer. Gene Ther 2003;10:1099-104.

78. Yant, S. R., Ehrhardt, A., Mikkelsen, J. G., et al. Transposition from a gutless adeno-transposon vector stabilizes transgene expression in vivo. Nat Biotechnol 2002;20:999-1005.

79. Yant, S. R., Meuse, L., Chiu, W., et al. Somatic integration and long-term transgene expression in normal and haemophilic mice using a DNA transposon system. Nat Genet 2000;25:35-41.

80. Huang, X., Wilber, A. C., Bao, L., et al. Stable gene transfer and expression in human primary T-cells by the Sleeping Beauty transposon system. Blood 2005;107:483-91.

81. Wilber, A., Linehan, J. L., Tian, X., et al. Efficient and stable transgene expression in human embryonic stem cells using transposon-mediated gene transfer. Stem Cells 2007;25:2919-27.

82. Collier, L. S., Carlson, C. M., Ravimohan, S., Dupuy, A. J., and Largaespada, D. A. Cancer gene discovery in solid tumours using transposon-based somatic mutagenesis in the mouse. Nature 2005;436:272-6.

83. Cui, Z., Geurts, A. M., Liu, G., Kaufman, C. D., and Hackett, P. B. Structure-function analysis of the inverted terminal repeats of the sleeping beauty transposon. J Mol Biol 2002;318:1221-35.

84. Izsvak, Z., Khare, D., Behlke, J., et al. Involvement of a bifunctional, paired-like DNA-binding domain and a transpositional enhancer in Sleeping Beauty transposition. J Biol Chem 2002;277:34581-8.

85. Karsi, A., Moav, B., Hackett, P., and Liu, Z. Effects of insert size on transposition efficiency of the sleeping beauty transposon in mouse cells. Mar Biotechnol (NY) 2001;3:241-5.

86. Lander, E. S., Linton, L. M., Birren, B., et al. Initial sequencing and analysis of the human genome. Nature 2001;409:860-921.

87. Zayed, H., Izsvak, Z., Khare, D., Heinemann, U., and Ivics, Z. The DNA-bending protein HMGB1 is a cellular cofactor of Sleeping Beauty transposition. Nucleic Acids Res 2003;31:2313-22.

88. Yant, S. R., Park, J., Huang, Y., Mikkelsen, J. G., and Kay, M. A. Mutational analysis of the N-terminal DNA-binding domain of sleeping beauty transposase: critical residues for DNA binding and hyperactivity in mammalian cells. Mol Cell Biol 2004;24:9239-47.

89. Zayed, H., Izsvak, Z., Walisko, O., and Ivics, Z. Development of hyperactive sleeping beauty transposon vectors by mutational analysis. Mol Ther 2004;9:292-304.

90. Chen, Z. J., Kren, B. T., Wong, P. Y., Low, W. C., and Steer, C. J. Sleeping Beauty-mediated down-regulation of huntingtin expression by RNA interference. Biochem Biophys Res Commun 2005;329:646-52.

91. Kaufman, C. D., Izsvák, Z., Katzer, A., and Ivics, Z. Frog Prince transposon-based RNAi vectors mediate efficient gene knockdown in human cells. Journal of RNAi and Gene Silencing 2005;1:97-104.

92. Craig, N. L. Unity in transposition reactions. Science 1995;270:253-4.

93. Doak, T. G., Doerder, F. P., Jahn, C. L., and Herrick, G. A proposed superfamily of transposase genes: transposon-like elements in ciliated protozoa and a common "D35E" motif. Proc Natl Acad Sci U S A 1994;91:942-6.

94. Izsvak, Z., Stuwe, E. E., Fiedler, D., et al. Healing the wounds inflicted by sleeping beauty transposition by double-strand break repair in mammalian somatic cells. Mol Cell 2004;13:279-90.

95. van Luenen, H. G., Colloms, S. D., and Plasterk, R. H. The mechanism of transposition of Tc3 in C. elegans. Cell. 1994;79:293-301.

96. Baus, J., Liu, L., Heggestad, A. D., Sanz, S., and Fletcher, B. S. Hyperactive transposase mutants of the Sleeping Beauty transposon. Mol Ther. 2005;12:1148-56. Epub 2005 Sep 8.

97. Walisko, O., Izsvak, Z., Szabo, K., et al. Sleeping Beauty transposase modulates cell-cycle progression through interaction with Miz-1. Proc Natl Acad Sci U S A. 2006;103:4062-7. Epub 2006 Mar 7.

98. Yant, S. R. and Kay, M. A. Nonhomologous-end-joining factors regulate DNA repair fidelity during Sleeping Beauty element transposition in mammalian cells. Mol Cell Biol 2003;23:8505-18.

99. Liu, G., Aronovich, E. L., Cui, Z., Whitley, C. B., and Hackett, P. B. Excision of Sleeping Beauty transposons: parameters and applications to gene therapy. J Gene Med 2004;6:574-83.

100. Yusa, K., Takeda, J., and Horie, K. Enhancement of Sleeping Beauty transposition by CpG methylation: possible role of heterochromatin formation. Mol Cell Biol 2004;24:4004-18.

101. Brenner, C. and Fuks, F. DNA methyltransferases: facts, clues, mysteries. Curr Top Microbiol Immunol 2006;301:45-66.

102. Liu, G., Geurts, A. M., Yae, K., et al. Target-site preferences of Sleeping Beauty transposons. J Mol Biol 2005;346:161-73.

103. Vigdal, T. J., Kaufman, C. D., Izsvak, Z., Voytas, D. F., and Ivics, Z. Common physical properties of DNA affecting target site selection of sleeping beauty and other Tc1/mariner transposable elements. J Mol Biol 2002;323:441-52.

104. Yant, S. R., Wu, X., Huang, Y., et al. High-resolution genome-wide mapping of transposon integration in mammals. Mol Cell Biol. 2005;25:2085-94.

105. Ivics, Z., Katzer, A., Stuwe, E. E., et al. Targeted Sleeping Beauty transposition in human cells. Mol Ther 2007;15:1137-44.

106. Wilber, A., Frandsen, J. L., Geurts, J. L., et al. RNA as a Source of Transposase for Sleeping Beauty-Mediated Gene Insertion and Expression in Somatic Cells and Tissues. Mol Ther 2005:Epub ahead of print.

107. Mikkelsen, J. G., Yant, S. R., Meuse, L., et al. Helper-Independent Sleeping Beauty transposon-transposase vectors for efficient nonviral gene delivery and persistent gene expression in vivo. Mol Ther 2003;8:654-65.

108. Hartl, D. L., Lohe, A. R., and Lozovskaya, E. R. Modern thoughts on an ancyent marinere: function, evolution, regulation. Annu Rev Genet 1997;31:337-58.

109. Tranchant, I., Thompson, B., Nicolazzi, C., Mignet, N., and Scherman, D. Physicochemical optimisation of plasmid delivery by cationic lipids. J Gene Med 2004;6 Suppl 1:S24-35.

110. Neu, M., Fischer, D., and Kissel, T. Recent advances in rational gene transfer vector design based on poly(ethylene imine) and its derivatives. J Gene Med 2005;7:992-1009.

111. Kaneda, Y., Yamamoto, S., and Nakajima, T. Development of HVJ Envelope Vector and Its Application to Gene Therapy. Adv Genet 2005:307-32.

112. Wolff, J. A. and Budker, V. The mechanism of naked DNA uptake and expression. Adv Genet 2005;54:3-20.

113. Greelish, J. P., Su, L. T., Lankford, E. B., et al. Stable restoration of the sarcoglycan complex in dystrophic muscle perfused with histamine and a recombinant adeno-associated viral vector. Nat Med 1999;5:439-43.

114. Dean, D. A. Nonviral gene transfer to skeletal, smooth, and cardiac muscle in living animals. Am J Physiol Cell Physiol 2005;289:C233-45.

115. Somiari, S., Glasspool-Malone, J., Drabick, J. J., et al. Theory and in vivo application of electroporative gene delivery. Mol Ther 2000;2:178-87.

116. Wells, D. J. Gene therapy progress and prospects: electroporation and other physical methods. Gene Ther 2004;11:1363-9.

117. Bowers, W. J., Mastrangelo, M. A., Howard, D. F., et al. Neuronal precursor-restricted transduction via in utero CNS gene delivery of a novel bipartite HSV amplicon/transposase hybrid vector. Mol Ther. 2006;13:580-8. Epub 2006 Jan 18.

118. Bell, J. B., Podetz-Pedersen, K. M., Aronovich, E. L., et al. Preferential delivery of the Sleeping Beauty transposon system to livers of mice by hydrodynamic injection. Nat Protoc 2007;2:3153-65.

119. Belur, L. R., Podetz-Pedersen, K., Frandsen, J., and McIvor, R. S. Lung-directed gene therapy in mice using the nonviral Sleeping Beauty transposon system. Nat Protoc 2007;2:3146-52.

120. Liu, F., Song, Y., and Liu, D. Hydrodynamics-based transfection in animals by systemic administration of plasmid DNA. Gene Ther 1999;6:1258-66.

121. Su, L. T., Gopal, K., Wang, Z., et al. Uniform scale-independent gene transfer to striated muscle after transvenular extravasation of vector. Circulation 2005;112:1780-8.

122. Feng, D. M., He, C. X., Miao, C. Y., et al. Conditions affecting hydrodynamics-based gene delivery into mouse liver in vivo. Clin Exp Pharmacol Physiol 2004;31:850-5.

123. Miao, C. H., Thompson, A. R., Loeb, K., and Ye, X. Long-term and therapeutic-level hepatic gene expression of human factor IX after naked plasmid transfer in vivo. Mol Ther 2001;3:947-57.

124. Zhang, G., Gao, X., Song, Y. K., et al. Hydroporation as the mechanism of hydrodynamic delivery. Gene Ther 2004;11:675-82.

125. Inoue, S., Hakamata, Y., Kaneko, M., and Kobayashi, E. Gene therapy for organ grafts using rapid injection of naked DNA: application to the rat liver. Transplantation 2004;77:997-1003.

126. Elouahabi, A. and Ruysschaert, J. M. Formation and intracellular trafficking of lipoplexes and polyplexes. Mol Ther 2005;11:336-47.

127. Lungwitz, U., Breunig, M., Blunk, T., and Gopferich, A. Polyethylenimine-based non-viral gene delivery systems. Eur J Pharm Biopharm 2005;60:247-66.

128. Boussif, O., Lezoualc'h, F., Zanta, M. A., et al. A versatile vector for gene and oligonucleotide transfer into cells in culture and in vivo: polyethylenimine. Proc Natl Acad Sci U S A 1995;92:7297-301.

129. Kopatz, I., Remy, J. S., and Behr, J. P. A model for non-viral gene delivery: through syndecan adhesion molecules and powered by actin. J Gene Med 2004;6:769-76.

130. Pollard, H., Toumaniantz, G., Amos, J. L., et al. Ca2+-sensitive cytosolic nucleases prevent efficient delivery to the nucleus of injected plasmids. J Gene Med 2001;3:153-64.

131. Goula, D., Becker, N., Lemkine, G. F., et al. Rapid crossing of the pulmonary endothelial barrier by polyethylenimine/DNA complexes. Gene Ther 2000;7:499-504.

132. Goula, D., Benoist, C., Mantero, S., et al. Polyethylenimine-based intravenous delivery of transgenes to mouse lung. Gene Ther 1998;5:1291-5.

133. Rudolph, C., Schillinger, U., Plank, C., et al. Nonviral gene delivery to the lung with copolymer-protected and transferrin-modified polyethylenimine. Biochim Biophys Acta 2002;1573:75-83.

134. Densmore, C. L. Polyethyleneimine-based gene therapy by inhalation. Expert Opin Biol Ther 2003;3:1083-92.

135. Boletta, A., Benigni, A., Lutz, J., et al. Nonviral gene delivery to the rat kidney with polyethylenimine. Hum Gene Ther 1997;8:1243-51.

136. Abdallah, B., Hassan, A., Benoist, C., et al. A powerful nonviral vector for in vivo gene transfer into the adult mammalian brain: polyethylenimine. Hum Gene Ther 1996;7:1947-54.

137. Coll, J. L., Chollet, P., Brambilla, E., et al. In vivo delivery to tumors of DNA complexed with linear polyethylenimine. Hum Gene Ther 1999;10:1659-66.

138. Godbey, W. T., Wu, K. K., and Mikos, A. G. Poly(ethylenimine)-mediated gene delivery affects endothelial cell function and viability. Biomaterials 2001;22:471-80.

139. Liu, L., Mah, C., and Fletcher, B. S. Sustained FVIII expression and phenotypic correction of hemophilia A in neonatal mice using an endothelial-targeted sleeping beauty transposon. Mol Ther 2006;13:1006-15.

140. Liu, H., Liu, L., Fletcher, B. S., and Visner, G. A. Novel action of indoleamine 2,3-dioxygenase attenuating acute lung allograft injury. Am J Respir Crit Care Med. 2006;173:566-72. Epub 2005 Nov 17.

141. Mukhopadhyay, A., Madhusudhan, T., and Kumar, R. Hematopoietic stem cells: clinical requirements and developments in ex-vivo culture. Adv Biochem Eng Biotechnol 2004;86:215-53.

142. Huard, J., Cao, B., and Qu-Petersen, Z. Muscle-derived stem cells: potential for muscle regeneration. Birth Defects Res C Embryo Today 2003;69:230-7.

143. Ozawa, C. R., Springer, M. L., and Blau, H. M. A novel means of drug delivery: myoblast-mediated gene therapy and regulatable retroviral vectors. Annu Rev Pharmacol Toxicol 2000;40:295-317.

144. Ferrari, S., Pellegrini, G., Mavilio, F., and De Luca, M. Gene therapy approaches for epidermolysis bullosa. Clin Dermatol 2005;23:430-6.

145. Ebert, A. D. and Svendsen, C. N. A new tool in the battle against Alzheimer's disease and aging: ex vivo gene therapy. Rejuvenation Res 2005;8:131-4.

146. Hacein-Bey-Abina, S., Von Kalle, C., Schmidt, M., et al. LMO2-associated clonal T cell proliferation in two patients after gene therapy for SCID-X1. Science 2003;302:415-9.

147. Huang, X., Guo, H., Kang, J., et al. Sleeping Beauty transposon-mediated engineering of human primary T cells for therapy of CD19+ lymphoid malignancies. Mol Ther 2008;16:580-9.

148. Hsu, C., Hughes, M. S., Zheng, Z., et al. Primary human T lymphocytes engineered with a codon-optimized IL-15 gene resist cytokine withdrawal-induced apoptosis and persist long-term in the absence of exogenous cytokine. J Immunol 2005;175:7226-34.

149. Pereboeva, L. and Curiel, D. T. Cellular vehicles for cancer gene therapy: current status and future potential. BioDrugs 2004;18:361-85.

150. Rossig, C., Bar, A., Pscherer, S., et al. Target antigen expression on a professional antigen-presenting cell induces superior proliferative antitumor T-cell responses via chimeric T-cell receptors. J Immunother 2006;29:21-31.

151. Rossig, C. and Brenner, M. K. Genetic modification of T lymphocytes for adoptive immunotherapy. Mol Ther 2004;10:5-18.

152. Zhang, D., Murakami, A., Johnson, R. P., et al. Optimization of ex vivo activation and expansion of macaque primary CD4-enriched peripheral blood mononuclear cells for use in anti-HIV immunotherapy and gene therapy strategies. J Acquir Immune Defic Syndr 2003;32:245-54.

153. Hacein-Bey-Abina, S., de Saint Basile, G., and Cavazzana-Calvo, M. Gene therapy of X-linked severe combined immunodeficiency. Methods Mol Biol 2003;215:247-59.

154. Dietrich, P. Y., Walker, P. R., Schnuriger, V., et al. TCR analysis reveals significant repertoire selection during in vitro lymphocyte culture. Int Immunol 1997;9:1073-83.

155. Zhou, X., Cui, Y., Huang, X., et al. Lentivirus-mediated gene transfer and expression in established human tumor antigen-specific cytotoxic T cells and primary unstimulated T cells. Hum Gene Ther 2003;14:1089-105.

156. Dupuy, A. J., Akagi, K., Largaespada, D. A., Copeland, N. G., and Jenkins, N. A. Mammalian mutagenesis using a highly mobile somatic Sleeping Beauty transposon system. Nature 2005;436:221-6.

157. Carlson, C. M., Frandsen, J. L., Kirchhof, N., McIvor, R. S., and Largaespada, D. A. Somatic integration of an oncogene-harboring Sleeping Beauty transposon models liver tumor development in the mouse. Proc Natl Acad Sci U S A 2005;102:17059-64.

158. Dalsgaard, T., Moldt, B., Sharma, N., et al. Shielding of sleeping beauty DNA transposon-delivered transgene cassettes by heterologous insulators in early embryonal cells. Mol Ther 2009;17:121-30.

159. Walisko, O., Schorn, A., Rolfs, F., et al. Transcriptional activities of the Sleeping Beauty transposon and shielding its genetic cargo with insulators. Mol Ther 2008;16:359-69.

160. Kaminski, J. M., Huber, M. R., Summers, J. B., and Ward, M. B. Design of a nonviral vector for site-selective, efficient integration into the human genome. Faseb J. 2002;16:1242-7.

161. Yew, N. S. and Cheng, S. H. Reducing the immunostimulatory activity of CpG-containing plasmid DNA vectors for non-viral gene therapy. Expert Opin Drug Deliv 2004;1:115-25.

162. Chen, Y., Lenert, P., Weeratna, R., et al. Identification of methylated CpG motifs as inhibitors of the immune stimulatory CpG motifs. Gene Ther. 2001;8:1024-32.

163. Reyes-Sandoval, A. and Ertl, H. C. CpG methylation of a plasmid vector results in extended transgene product expression by circumventing induction of immune responses. Mol Ther. 2004;9:249-61.

164. Gallo-Penn, A. M., Shirley, P. S., Andrews, J. L., et al. Systemic delivery of an adenoviral vector encoding canine factor VIII results in short-term phenotypic correction, inhibitor development, and biphasic liver toxicity in hemophilia A dogs. Blood 2001;97:107-13.

165. Ye, P., Thompson, A. R., Sarkar, R., et al. Naked DNA transfer of factor VIII induced transgene-specific, species-independent immune response in hemophilia A mice. Mol Ther 2004;10:117-26.

166. Williams, D. A. Sleeping beauty vector system moves toward human trials in the United States. Mol Ther 2008;16:1515-6.

167. Kichler, A. Gene transfer with modified polyethylenimines. J Gene Med 2004;6 Suppl 1:S3-10.

168. Wilson, M. H., Kaminski, J. M., and George, A. L., Jr. Functional zinc finger/sleeping beauty transposase chimeras exhibit attenuated overproduction inhibition. FEBS Lett 2005;579:6205-9.

169. Ohlfest, J. R., Lobitz, P. D., Perkinson, S. G., and Largaespada, D. A. Integration and long-term expression in xenografted human glioblastoma cells using a plasmid-based transposon system. Mol Ther 2004;10:260-8.

170. Wu, A., Oh, S., Ericson, K., et al. Transposon-based interferon gamma gene transfer overcomes limitations of episomal plasmid for immunogene therapy of glioblastoma. Cancer Gene Ther 2007;14:550-60.

171. Holliger, P. and Hudson, P. J. Engineered antibody fragments and the rise of single domains. Nat Biotechnol. 2005;23:1126-36.

172. Colcher, D., Pavlinkova, G., Beresford, G., Booth, B. J., and Batra, S. K. Single-chain antibodies in pancreatic cancer. Ann N Y Acad Sci. 1999;880:263-80.

173. Xu, X., Clarke, P., Szalai, G., et al. Targeting and therapy of carcinoembryonic antigen-expressing tumors in transgenic mice with an antibody-interleukin 2 fusion protein. Cancer Res 2000;60:4475-84.

174. Ran, S., Gao, B., Duffy, S., et al. Infarction of solid Hodgkin's tumors in mice by antibody-directed targeting of tissue factor to tumor vasculature. Cancer Res. 1998;58:4646-53.

175. Kaspar, M., Trachsel, E., and Neri, D. The antibody-mediated targeted delivery of interleukin-15 and GM-CSF to the tumor neovasculature inhibits tumor growth and metastasis. Cancer Res 2007;67:4940-8.

176. Ruf, W., Rehemtulla, A., Morrissey, J. H., and Edgington, T. S. Phospholipid-independent and -dependent interactions required for tissue factor receptor and cofactor function. J Biol Chem. 1991;266:2158-66.

177. Davie, E. W., Fujikawa, K., and Kisiel, W. The coagulation cascade: initiation, maintenance, and regulation. Biochemistry. 1991;30:10363-70.

178. Tilley, R. and Mackman, N. Tissue factor in hemostasis and thrombosis. Semin Thromb Hemost. 2006;32:5-10.

179. Huang, X., Molema, G., King, S., et al. Tumor infarction in mice by antibody-directed targeting of tissue factor to tumor vasculature. Science. 1997;275:547-50.

180. Nilsson, F., Kosmehl, H., Zardi, L., and Neri, D. Targeted delivery of tissue factor to the ED-B domain of fibronectin, a marker of angiogenesis, mediates the infarction of solid tumors in mice. Cancer Res. 2001;61:711-6.

181. Chen, K. H., Liu, S., Bankston, L. A., Liddington, R. C., and Leppla, S. H. Selection of anthrax toxin protective antigen variants that discriminate between the cellular receptors TEM8 and CMG2 and achieve targeting of tumor cells. J Biol Chem 2007;282:9834-45.

182. Kessler, T., Bieker, R., Padro, T., et al. Inhibition of tumor growth by RGD peptide-directed delivery of truncated tissue factor to the tumor vasculature. Clin Cancer Res 2005;11:6317-24.

183. Lamikanra, A., Myers, K. A., Ferris, N., Mitrophanous, K. A., and Carroll, M. W. In vivo evaluation of an EIAV vector for the systemic genetic delivery of therapeutic antibodies. Gene Ther 2005;12:988-98.

184. Taft, S. C. and Weiss, A. A. Toxicity of anthrax toxin is influenced by receptor expression. Clin Vaccine Immunol 2008;15:1330-6.

185. Bagley, R. G., Rouleau, C., St Martin, T., et al. Human endothelial precursor cells express tumor endothelial marker 1/endosialin/CD248. Mol Cancer Ther 2008;7:2536-46.

186. Gao, D., Nolan, D. J., Mellick, A. S., et al. Endothelial progenitor cells control the angiogenic switch in mouse lung metastasis. Science 2008;319:195-8.

187. Lyden, D., Hattori, K., Dias, S., et al. Impaired recruitment of bone-marrow-derived endothelial and hematopoietic precursor cells blocks tumor angiogenesis and growth. Nat Med 2001;7:1194-201.

188. Peters, B. A., Diaz, L. A., Polyak, K., et al. Contribution of bone marrow-derived endothelial cells to human tumor vasculature. Nat Med 2005;11:261-2.

BIOGRAPHICAL SKETCH

Stephen John Fernando was born in the small town of Glen Carbon, Illinois. He graduated high school in 1997, and took an interest in science when he attended Southern Illinois University at Edwardsville. In 2001, he graduated from the University of Illinois at Urbana-Champaign with a Microbiology Degree and took various jobs at biotechnology firms in Chicago, Illinois. In 2004, he decided to continue his education in warmer areas of the country and matriculated into the Interdisciplinary Program of Biomedical Sciences at the University of Florida. In the spring of 2005, he joined the lab of Dr. Bradley Fletcher and began work on a cancer therapy that specifically targeted the protein TEM8. He received his Ph.D. for this work from the University of Florida in the Spring of 2009. His work at the time of graduation was in press at the prestigous journal Cancer Research.